The first *wave theory* RTM, examples with a layered medium, predicting the source and receiver at depth and then imaging, providing the correct location and reflection amplitude at every depth location, and where the data includes primaries and all internal multiples.

Fang Liu and Arthur B. Weglein

April 29, 2013

Abstract

Reverse time migration (RTM) is the cutting-edge imaging method used in seismic exploration. In earlier RTM publications, density was often used to balance a medium with velocity variation, such that the acoustic impedance − the product of velocity and density − stays constant. Thus, reflections from sharp boundaries are avoided. In order to be more complete, consistent, realistic, and predictive, density variation is intentionally included in our study so that we can test its impact on the Green's theorem-based wave-theory RTM algorithms.

The major objectives of this article are to advance our understanding and to provide concepts, added imaging capabilities, and new algorithms for RTM. Although our objective of extracting useful subsurface information from recorded data is not different from that of well-known previous RTM publications, our approach is different: we use wave theory as much as possible to maximize the benefit from the Green's function and Green's theorem, rather than use the more popular methodology of running finite-difference modeling backwards in time.

A significant artifact in RTM is caused by the fact that numerous subsurface seismic events necessary for backward propagation never return to the measurement surface. This unwanted phenomenon also exists for the wave-field-prediction method formulated from Green's theorem: Green's formula (in its general form, i.e., equation (2.5)), which links the wave field on the entire outer surface with interior field values, also requires data from everywhere on the surface. Weglein et al. (2011a) and Weglein et al. (2011b) proposed a special Green's function with vanishing Dirichlet and Neumann boundary conditions at the deeper boundary to cope with that issue. This article provides a natural extension of the two aforementioned papers, into a medium with density variation and more complicated geological structures.

The major advantage of RTM over many other seismic imaging methods is its additional ability to handle two-way propagation without assuming that the events in the input data are only up-going and that all multiples have been removed. This article demonstrates with numerical examples that both up- and down-going waves can be precisely predicted from the data (including internal multiples) on the top surface only. In our example, the contribution of the transmission events that never return to the measurement surface is deliberately eliminated, and it is not necessary for those events to enter the calculation.

The Green's function with vanishing Dirichlet and Neumann boundary conditions at the deeper boundary demonstrates many remarkable properties. For example, it vanishes if the receiver is deeper than the source, it violates reciprocity, and its value is not affected by any heterogeneity outside the region between the source and receiver. The double vanishing boundary condition also leads us to a wave-theory solution for a model that has many reflectors and lacks internal multiples.

In this paper, two approaches have been used to derive the Green's function with vanishing Dirichlet and Neumann boundary conditions at the deeper boundary. The first is an analytical boundary-matching method in the frequency domain, and the second is the numerical finite-difference approach identical to many current finite-difference forward-modeling procedures in the industry. The second method can be extended to multiple dimensions with lateral variation in the medium properties. We find these two methods agree with each other with regard to the intrinsic accuracy issue of the finite-difference approximation to differential equations.

In this paper, we also have some very early and very positive news on the first wave theory RTM imaging tests, with a discontinuous reference medium and images that have the correct depth and amplitude (that is, producing the reflection coefficient at the correctly located target) with primaries and multiples in the data. That is an implementation of Weglein et al. (2011a;b) with creative implementation and testing and analysis.

1 Introduction

One of the major early objectives of Reverse Time Migration (RTM) is to obtain a better image of salt flanks through diving waves than is obtained by directly imaging through the complex overburden. The key new capability of the RTM method compared with one-way migration algorithms is to allow two-way wave propagation in the imaging procedure. This article follows closely the idea established in Weglein et al. (2011a;b): achieving a Green's function with vanishing Dirichlet and Neumann boundary conditions at the deeper boundary, to eliminate the need for measurement at depth.

To achieve the two-way imaging, we study the behavior of our Green's function in three examples: (1) a homogeneous model, (2) a single reflector model, and (3) a two-reflector model with internal multiples. In order to get two-way propagation without complexity and approximation, we study 1D examples with both up- and down-going wave propagation. We provide the details to demonstrate the underlying physics.

As stated in Whitmore (1983); Baysal et al. (1983); Luo and Schuster (2004); Fletcher et al. (2006); Liu et al. (2009) and Vigh et al. (2009), accurate medium properties above the target are required for the RTM procedure discussed in this article. The major difference is that in most RTM algorithms in the industry, a smoothed version of the velocity is used in the imaging procedure to avoid reflections from the velocity model itself, while the exact velocity models (often discontinuous) are used in all three examples in this article.

To apply the firm footing and math-physics foundation established in Weglein et al. (2011a;b) in an arbitrary medium, we first study in detail the properties of the Green's functions with vanishing boundary conditions at the deeper boundary $z' = \mathcal{B}$. The understanding of the aforementioned properties provides us with a straightforward procedure for constructing a Green's function with the double vanishing boundary condition for a 1D medium with arbitrary complexity. We adopt the notations of the aforementioned articles as much as possible while introducing some minor modifications to allow smooth expansions into new territories.

One of the remarkable properties of the Green's function in this article is that, although both the causal Green's function G_0^+ and the anti-causal Green's function G_0^- vary with the medium below the source, the Green's function with both vanishing Dirichlet and Neumann boundary conditions does not. The implications are that if we want to predict the wave field at depth z, the medium's properties deeper than z are not required. Such a property is very difficult to visualize if G_0^+ or G_0^- is used to make the prediction, since both of them will change with the medium's properties deeper than z. It is worthwhile to note that this property of the Green's function with vanishing boundary conditions is also demonstrated by the WKBJ Green's function used in the derivation of FK and phase-shift migrations. While the WKBJ Green's function is an approximate solution for a medium with smooth variations, and the Green's function with double vanishing boundary conditions in this report is exact and for a discontinuous medium, nevertheless we find their similarity worth reporting.

The property that allows an easy iterative procedure for constructing a Green's function with double vanishing boundary conditions is the following: the field values of the Green's function vanishing at the deeper surface are not affected by heterogeneity beyond the region between the field point and the source. Consequently, we can start the calculation from a field location sufficiently close to the source that the medium in between is homogeneous. In this case, the initial field value (for all time and frequency values) can be calculated from a much simpler medium obtained by extending the homogeneity to the entire space*. This initial field value contains two parts: the first part† is the out-going G_0^+ and is produced by the actual source, and the second term is the downward propagation portion‡ that will cancel with the downward propagation energy of G_0^+. Consequently, it will give a solution that vanishes completely below the source, satisfying both Dirichlet and Neumann boundary conditions. For the solution of the wave field above the initial field, standard analytic boundary-matching methods or discrete finite-difference procedures can be used to iteratively extrapolate the function values to locations further and further away from the source location.

Another property of the Green's function with both Dirichlet and Neumann boundary conditions vanishing is that it contains no multiples or reflections from the energy produced by the source, even for models with an arbitrary number of reflectors. This property, derived from precise Green's theory, agrees with many methodologies in the current seismic imaging procedures (which are often derived with some approximation to the wave equation): a smooth model is preferred, in order to exclude reflections and multiples caused by the velocity model.

The major contributions of this article are:

*For example, equation (14) of Weglein et al. (2011b) or equation (3.1) in this paper.

†The second term of equation (14) of Weglein et al. (2011b).

‡The first term of equation (14) of Weglein et al. (2011b).

- It provides two methods to calculate the Green's function with vanishing Dirichlet and Neumann boundary conditions for arbitrary 1D medium.
- It incorporates the density variation for Green's theorem RTM.
- It provides the finite-difference scheme for calculating the Green's function that vanishes at the deeper boundary.
- It provides a two-way propagation and downward continuation of wave fields, by using Green's function with double vanishing boundary conditions.
- It demonstrates remarkable properties of the precise analytical Green's function that coincide with many existing seismic imaging ideas derived with different degrees of approximation.

The following notations are worth mentioning at the beginning: G_0^+ and G_0^- are used to denote causal and anti-causal Green's functions, respectively. G_0^{DN} is used to denote the Green's function with vanishing Dirichlet and Neumann boundary conditions at the deeper boundary. $k = \omega/c_0$ where c_0 is the constant velocity of the reference medium, and ω is the angular frequency.

Although Green's theorem and Green's functions are more often discussed in the frequency domain, in this paper the Green's functions and wave field prediction examples are always graphed in the time domain since this domain is more easily accessible (without expressing the values in complex numbers). A very straightforward Fourier transform is sufficient to make the domain change:

$$f(t) = \frac{1}{2\pi} \int_{-\infty}^{\infty} \widetilde{f}(\omega) e^{-i\omega t} d\omega. \tag{1.1}$$

The Green's function, resulting from an ideal impulsive source, contains frequency information of an arbitrary frequency. For display, we convolve it with a band-limited wavelet (the first derivative of a Gaussian function[§]) to avoid aliasing beyond the Nyquist frequency.

2 Green's theorem wave-field prediction with density variation

In many migration methods, density variation is often left out of the acoustic wave equation since it does not affect the travel time. In reverse time migration, however, density serves a very important role even in the early stage: in order to have a reflectionless medium with velocity variations, a counterbalancing density variation is introduced to make sure the acoustic impedance is constant. Therefore in our derivation of Green's theorem-based RTM, we explicitly incorporate the density variations in the acoustic medium. First, let us assume the wave propagation problem in a volume V bounded by a shallower depth $\mathcal{A}$ and deeper depth $\mathcal{B}$:

[§]The wavelet is $i\omega e^{-\omega^2/\beta}$ in the frequency domain or $\frac{1}{2}\sqrt{\frac{\beta}{\pi}} e^{-\beta t^2/4}$ in the time domain, where $\beta = (20\pi)^2$

$$\left\{\frac{\partial}{\partial z'}\frac{1}{\rho(z')}\frac{\partial}{\partial z'}+\frac{\omega^2}{\rho(z')c^2(z')}\right\}P(z',\omega)=0 \quad , \quad \mathcal{A}<z'<\mathcal{B}, \tag{2.1}$$

where z' is the depth, and $\rho(z')$ and $c(z')$ are the density and velocity fields, respectively. In exploration seismology, we let the shallower depth $\mathcal{A}$ be the measurement surface where the seismic acquisition can be accomplished economically. The volume V is the finite volume defined in the "finite volume model" for migration, the details of which can be found in Weglein et al. (2011a). We measure P at the measurement surface $z'=\mathcal{A}$, and the objective is to predict P anywhere between the shallower surface and another surface with greater depth, $z'=\mathcal{B}$. This can be achieved via the solution of the wave-propagation equation in the same medium by an idealized impulsive source or Green's function:

$$\left\{\frac{\partial}{\partial z'}\frac{1}{\rho(z')}\frac{\partial}{\partial z'}+\frac{\omega^2}{\rho(z')c^2(z')}\right\}G_0(z,z',\omega)=\delta(z-z') \quad , \quad \mathcal{A}<z'<\mathcal{B}, \tag{2.2}$$

where z is the location of the source, and z' and z increase in a downward direction. It can be achieved as follows:

- Multiply equation (2.2) by $P(z',\omega)$.
- Multiply equation (2.1) by $G_0(z,z',\omega)$.
- Integrate the difference of the two aforementioned products (both are functions of z') over the variable z' from $\mathcal{A}$ to $\mathcal{B}$.

The right-hand side of the operation above is:

$$\int_{\mathcal{A}}^{\mathcal{B}} P(z',\omega)\delta(z-z')dz' = P(z,\omega), \tag{2.3}$$

where in the derivation above we assume z is inside the volume V (i.e., $\mathcal{A}<z<\mathcal{B}$). Omitting the arguments of the following functions: $P(z',\omega)$, $G_0(z,z',\omega)$, $c(z')$ and $\rho(z')$, since their arguments will not be changed in the derivation process, the left-hand side of the operation above is:

$$
\begin{aligned}
&\int_{\mathcal{A}}^{\mathcal{B}} \left[P\frac{\partial}{\partial z'}\left\{\frac{1}{\rho}\frac{\partial G_0}{\partial z'}\right\} + \frac{\omega^2 P G_0}{\rho c^2} - G_0\frac{\partial}{\partial z'}\left\{\frac{1}{\rho}\frac{\partial P}{\partial z'}\right\} - \frac{\omega^2 P G_0}{\rho c^2}\right] dz' \\
=&\int_{\mathcal{A}}^{\mathcal{B}} \left[P\frac{\partial}{\partial z'}\left\{\frac{1}{\rho}\frac{\partial G_0}{\partial z'}\right\} - G_0\frac{\partial}{\partial z'}\left\{\frac{1}{\rho}\frac{\partial P}{\partial z'}\right\}\right] dz' \\
=&\int_{\mathcal{A}}^{\mathcal{B}} \left[P\frac{\partial}{\partial z'}\left\{\frac{1}{\rho}\frac{\partial G_0}{\partial z'}\right\} + \frac{\partial P}{\partial z'}\frac{1}{\rho}\frac{\partial G_0}{\partial z'} - G_0\frac{\partial}{\partial z'}\left\{\frac{1}{\rho}\frac{\partial P}{\partial z'}\right\} - \frac{\partial G_0}{\partial z'}\frac{1}{\rho}\frac{\partial P}{\partial z'}\right] dz' \\
=&\int_{\mathcal{A}}^{\mathcal{B}} \left[\frac{\partial}{\partial z'}\left\{\frac{P}{\rho}\frac{\partial G_0}{\partial z'}\right\} - \frac{\partial}{\partial z'}\left\{\frac{G_0}{\rho}\frac{\partial P}{\partial z'}\right\}\right] dz' = \int_{\mathcal{A}}^{\mathcal{B}} \frac{\partial}{\partial z'}\left\{\frac{P}{\rho}\frac{\partial G_0}{\partial z'} - \frac{G_0}{\rho}\frac{\partial P}{\partial z'}\right\} dz' \\
=&\int_{\mathcal{A}}^{\mathcal{B}} \frac{\partial}{\partial z'}\left\{\frac{1}{\rho}\left[P\frac{\partial G_0}{\partial z'} - G_0\frac{\partial P}{\partial z'}\right]\right\} dz' \\
=&\frac{1}{\rho}\left\{P\frac{\partial G_0}{\partial z'} - G_0\frac{\partial P}{\partial z'}\right\}\Bigg|_{z'=\mathcal{A}}^{z'=\mathcal{B}}.
\end{aligned}
\tag{2.4}
$$

Equating the results obtained by the left- and right-hand-side operations, and restoring the specific arguments of each function, we have:

$$
P(z,\omega) = \frac{1}{\rho(z')}\left\{P(z',\omega)\frac{\partial G_0(z,z',\omega)}{\partial z'} - G_0(z,z',\omega)\frac{\partial P(z',\omega)}{\partial z'}\right\}\Bigg|_{z'=\mathcal{A}}^{z'=\mathcal{B}}, \tag{2.5}
$$

where $\mathcal{A}$ and $\mathcal{B}$ are the shallower and deeper boundaries, respectively, of the volume to which the Green's theorem is applied. It is identical to equation (43) of Weglein et al. (2011a), except for the additional density contribution to the Green's theorem. Similar density contributions can be found in many seismic imaging procedures, such as equation (21) of Clayton and Stolt (1981).

In the arguments of G_0, z is the location of the source, and z' is the location of the receiver. The Green's theorem given in equation (2.5) predicts the data $P(z,\omega)$ in an arbitrary location using the data $P(z',\omega)$ at the measurement surface. In this specific application, z is the depth at which the wave-field prediction is carried out.

Note that in equation (2.5), the field values at the surface of the volume V are necessary for predicting the field value inside V. The surface of V contains two parts: the shallower portion $z' = \mathcal{A}$ and the deeper portion $z' = \mathcal{B}$. In seismic exploration, the need for data at $z' = \mathcal{B}$ is often the issue. For example, one of the significant artifacts of the current RTM procedures is caused by

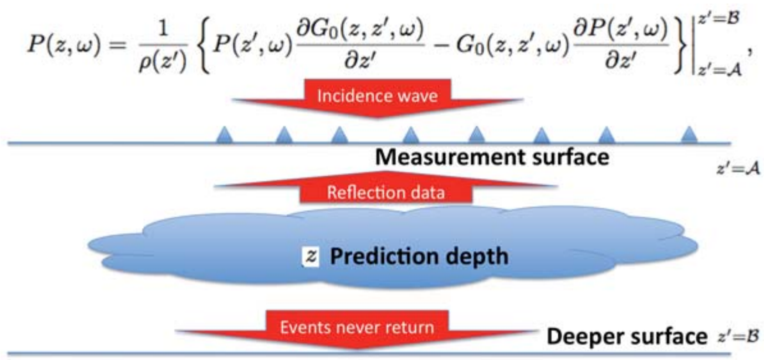

Figure 1: Green's theorem predicts the wave field at an arbitrary depth z between the shallower depth $\mathcal{A}$ and deeper depth $\mathcal{B}$.

this phenomenon: there are events necessary for accurate wave-field prediction that reach $z' = \mathcal{B}$ but never return to $z' = \mathcal{A}$, as is demonstrated in Figure 1. The solution, based on Green's theorem without any approximation, was first published in Weglein et al. (2011a) and Weglein et al. (2011b), the basic idea can be summarized as the following.

Since the wave equation is a second-order differential equation, its solution is not unique. In other words, for a wave equation with a specific medium property, there are an infinite number of solutions. This freedom in choosing the Green's function has been taken advantage of in many seismic-imaging procedures. For example, the most popular choice in wave-field prediction is the physical solution G_0^+. In downward continuing an up-going wave field to a subsurface, the anti-causal solution G_0^- is often used.

If both G_0 and $\partial G_0/\partial z'$ vanish at the deeper boundary $z' = \mathcal{B}$, where measurement is often much more expensive than acquiring data at the shallower boundary $z' = \mathcal{A}$, then only the data at the shallower surface (i.e., the actual measurement surface) is needed in the calculation. We use G_0^{DN} to denote the Green's function with vanishing Dirichlet and Neumann boundary conditions at the deeper boundary.

3 The vanishing property of G_0^{DN} and its independence of the medium's properties below the source

First, let us look at some properties of the Green's function detailed in equation (14) of Weglein et al. (2011b):

$$G_0^{DN}(z, z', \omega) = \frac{-1}{2ik}\left(e^{-ik(z-z')} - e^{ik|z-z'|}\right), \tag{3.1}$$

where $k = \omega/c_0$ and the quantity c_0 is the unchanged homogeneous velocity in the entire space, and z and z' are the locations of the source and receiver, respectively. This Green's function is

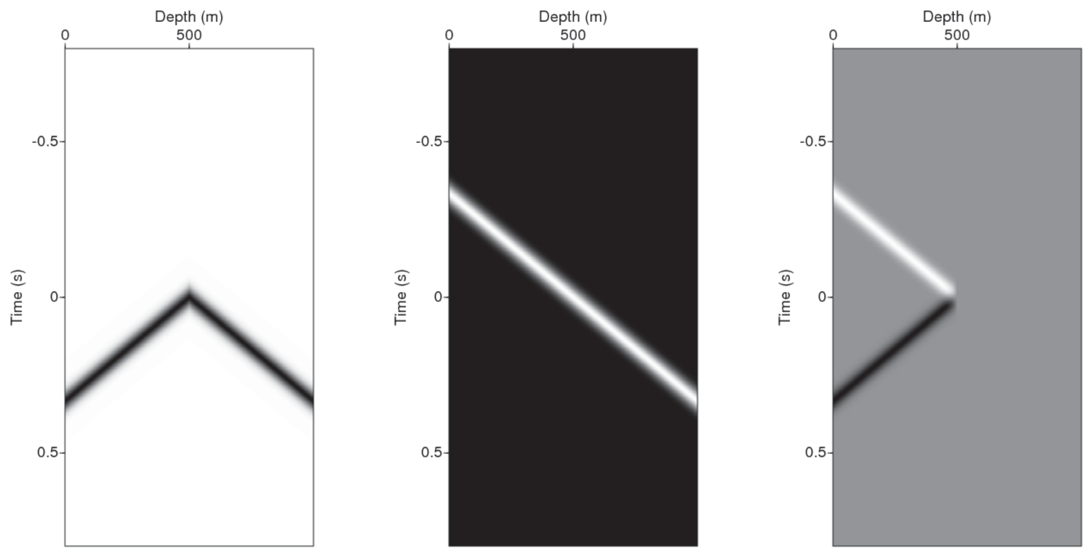

Figure 2: The construction of G_0^{DN} for a homogeneous medium with constant velocity $1500m/s$. The source depth is 500m. The left panel is the causal solution (if we denote $k = \omega/c_0$ and H is the Heaviside function, the causal Green's function is $G_0^+(z, z', \omega) = e^{ik|z-z'|}/(2ik)$ in the frequency domain or $G_0^+(z, z', t) = \frac{-c_0}{2}H(t - |z - z'|/c_0)$ in the time domain). The middle panel shows the homogeneous solution ($-e^{ik(z'-z)}/(2ik)$ in the frequency domain or $\frac{c_0}{2}H(t-(z'-z)/c_0)$ in the time domain) that cancels with the left panel below the source. The right panel results from summing the two panels on its left and is the desired Green's function with double vanishing boundary conditions.

for a whole-space homogeneous medium with c_0 as its velocity. It also satisfies the Dirichlet and Neumann boundary conditions at the deeper boundary $\mathcal{B}$:

$$G_0^{DN}(z,z',\omega)\big|_{z'=\mathcal{B}} = 0,$$
$$\left.\frac{\partial G_0^{DN}(z,z',\omega)}{\partial z'}\right|_{z'=\mathcal{B}} = 0.$$

The construction of equation (3.1) (i.e., G_0^{DN} in a homogeneous medium) is detailed in Weglein et al. (2011b); we only provide its graphic version in this article in Figure 2.

In equation (3.1), the second term is the causal solution for the same homogeneous medium, and the first term is a specific solution to the homogeneous¶ wave equation, introduced to perfectly cancel the causal solution at the deeper boundary. The major objective of this Green's function is to eliminate the need for measurement at the deeper surface: $z' = \mathcal{B}$.

According to equation (2.5), for arbitrary values of the wave field $P(z',\omega)$, this objective implies $G_0(z,z',\omega)|_{z'=\mathcal{B}} = \left.\frac{\partial G_0(z,z',\omega)}{\partial z'}\right|_{z'=\mathcal{B}} = 0$, since normally the data are available only at the measurement surface: $z' = \mathcal{A}$. The variable z is used to denote the depth to which we want to continue the wave field downward. It is obvious that $\mathcal{A} < z' < \mathcal{B}$. First, if $z < z'$, this Green's operator vanishes, since

$$\begin{aligned} G_0^{DN}(z,z',\omega) &= \frac{-1}{2ik}\left(e^{-ik(z-z')} - e^{ik|z-z'|}\right) \\ &\overset{z<z'}{=} \frac{-1}{2ik}\left(e^{ik(z'-z)} - e^{ik(z'-z)}\right) \\ &\equiv 0. \end{aligned} \tag{3.2}$$

According to equation (3.2), this Green's function vanishes not only for the isolated location at $\mathcal{B}$, but also in the extended entire half-space below the source, which include $z' = \mathcal{B}$.

Obviously this Green's function satisfies the wave equation of the whole-space homogeneous medium (i.e., equation (7) of Weglein et al. (2011b)):

$$\left(\frac{d^2}{dz'^2} + \frac{\omega^2}{c_0^2}\right) G_0^{DN}(z,z',\omega) = \delta(z-z'). \tag{3.3}$$

If we have an inhomogeneous medium $c(z')$ such that $c(z') = c_0$ when $z' < z$, the Helmholtz equation for this inhomogeneous medium is

¶In this article the adjective homogeneous has different meaning when it acts on medium or equation. In the first case it means medium with constant acoustic property in the entire space, while in the second case it means a wave equation without the source term.

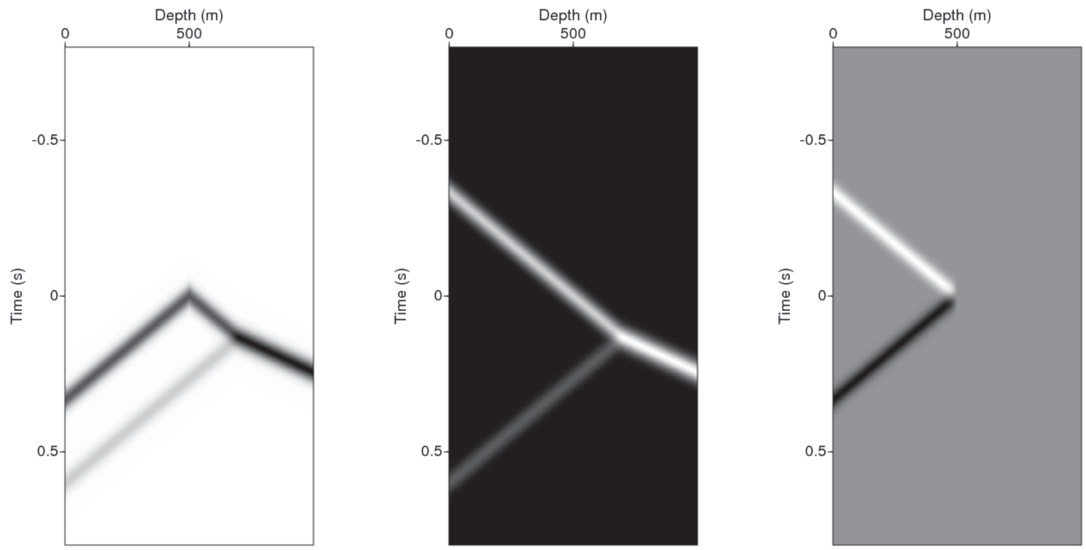

Figure 3: The construction of G_0^{DN} for a medium with one reflector (the velocities above and below the reflector are $1500m/s$ and $2700m/s$, respectively). The source depth is 500m and is above the single reflector at $700m$. The left panel is the causal solution G_0^+, and the middle panel shows the homogeneous solution that cancels with the left panel below the source. The right panel results from summing the two panels on its left and is the desired Green's function with double vanishing boundary conditions.

$$\left(\frac{d^2}{dz'^2} + \frac{\omega^2}{c^2(z')}\right) \mathcal{G}_0(z, z', \omega) = \delta(z - z'). \tag{3.4}$$

When $z' < z$, wave equation (3.4) is satisfied by Green's function (3.1) since it satisfies the homogeneous wave equation (3.3), which is identical to the inhomogeneous equation (3.4) when $z' < z$.

For the other possibility, that $z' > z$, wave equation (3.4) is also satisfied by Green's function (3.1) since it completely vanishes in this region. If we substitute G_0^{DN} for $\mathcal{G}_0$, left-hand side of equation (3.4) vanishes since the spatial partial derivative is zero, while the right-hand side vanishes due to the fact that the source z is located outside the region of interest. Consequently, equation (3.4) is satisfied by the Green's function in equation (3.3).

As an example, introducing a single reflector below the source for the Green's function in equation (16) of Weglein et al. (2011b) will not change the value of the Green's function. The construction of G_0^{DN} with its source located above the single reflector is detailed in Weglein et al. (2011b); here we provide its graphical version in Figure 3. The equivalence of the Green's function (3.1) to equation (39) in Weglein et al. (2011b) can be demonstrated as follows. Since a is the depth of the reflector, and we consider the case in which the source is above the reflector, we have $z < a$ and $\texttt{sgn}(a - z) = 1$. According to Appendix B of Weglein et al. (2011b), we have: $D_1 = 0$, $C_1 = -\frac{T}{2ik}e^{ik|a-z|}e^{-ik_1 a} = -\frac{T}{2ik}e^{ik(a-z)}e^{-ik_1 a}$. Thus, the wave field below the reflector (i.e., $z' > a$, the transmitted wave) can be simplified as:

$$
\begin{aligned}
&\frac{T}{2ik}e^{ik|a-z|}e^{ik_1(z'-a)} + C_1 e^{ik_1 z'} + D_1 e^{-ik_1 z'} \\
=&\frac{T}{2ik}e^{ik|a-z|}e^{ik_1(z'-a)} - \frac{T}{2ik}e^{ik|a-z|e^{-ik_1 a}}e^{ik_1 z'} + 0 \times e^{-ik_1 z'} \\
=&\frac{T}{2ik}e^{ik|a-z|}e^{ik_1(z'-a)} - \frac{T}{2ik}e^{ik|a-z|}e^{ik_1(z'-a)} \equiv 0.
\end{aligned}
\tag{3.5}
$$

Obviously, this Green's function vanishes if $z' > a$ (is deeper than the reflector). The same vanishing property is also displayed for G_0^{DN} without the single reflector below the source; the details can be found in equation (3.2).

Since $A_1 = \frac{-1}{2ik}e^{-ikz}$, and $B_1 = \frac{-R}{2ik}e^{ik(2a-z)}$, and if $z' < a$ is above the reflector, the reflected wave in equation (39) of Weglein et al. (2011b) can be simplified as follows:

$$
\begin{aligned}
&\frac{e^{ik|z'-z|}}{2ik} + R\frac{e^{-ik(z'-a)}}{2ik}e^{ik(a-z)} + A_1 e^{ikz'} + B_1 e^{-ikz'} \\
=&\frac{e^{ik|z'-z|}}{2ik} + R\frac{e^{ik(2a-z'-z)}}{2ik} + A_1 e^{ikz'} + B_1 e^{-ikz'} \\
=&\frac{e^{ik|z'-z|}}{2ik} + R\frac{e^{ik(2a-z'-z)}}{2ik} - \frac{e^{ik(z'-z)}}{2ik} - \frac{R}{2ik}e^{ik(2a-z)}e^{-ikz'} \\
=&\frac{e^{ik|z'-z|}}{2ik} + R\frac{e^{ik(2a-z'-z)}}{2ik} - \frac{e^{ik(z'-z)}}{2ik} - R\frac{e^{ik(2a-z'-z)}}{2ik} \\
=&\frac{e^{ik|z'-z|}}{2ik} - \frac{e^{ik(z'-z)}}{2ik} = \frac{-1}{2ik}\left(e^{ik(z'-z)} - e^{ik|z'-z|}\right).
\end{aligned}
\tag{3.6}
$$

Consequently, it is identical to the Green's function (3.1) for $z' < a$ (i.e., to equation (14) of Weglein et al. (2011b), the Green's function with the same vanishing Dirichlet and Neumann boundary conditions at the deeper boundary for a whole-space homogeneous medium). In other words, the reflector below the source will not change the values of the Green's function with vanishing Dirichlet and Neumann boundary conditions at the deeper boundary.

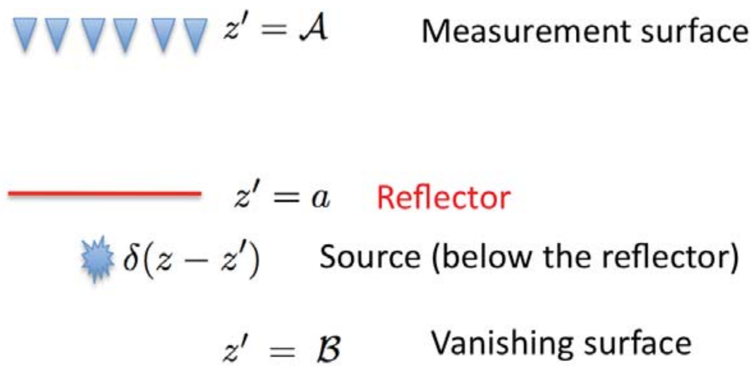

Figure 4: The configuration of the experiment with the source below a single reflector.

4 G_0^{DN} for a model with a single reflector

4.1 Case I: source above the reflector

This case had been derived and documented in detail in Weglein et al. (2011b). The only additional contribution we have in this article is the density term in the amplitude of the Green's function:

$$G_0^{DN}(z, z', \omega) = \frac{\rho_0}{2ik}\left(e^{ik|z-z'|} - e^{-ik(z-z')}\right). \tag{4.1}$$

In the equation above, the density at the source location is the extra contribution in extending the Green's function in equation (39) of Weglein et al. (2011b). A similar density term can be found in the Green's function of Clayton and Stolt (1981).

We can also Fourier transform equation (4.1) to the time domain to have:

$$G_0^{DN}(z, z', t) = \frac{\rho_0 c_0}{2}\left(H\left[t - \frac{z'-z}{c_0}\right] - H\left[t - \frac{|z'-z|}{c_0}\right]\right). \tag{4.2}$$

4.2 Case II: source below the reflector

From the previous section, if $z < a$, the solution is trivial since $G_0^{DN}(z, z', \omega) = G_0^{DN}(z, z', \omega)$. It is critical to derive G_0^{DN} for $z > a$. The physical experiment is the following (see Figure 4): The locations of the measurement surface and the deeper surface are $\mathcal{A}$ and $\mathcal{B}$, respectively. The depth of the single reflector and source are a and z, respectively. The causal Green's function with the source located at depth z and receiver at depth z' is denoted as $G_0^+(z, z', \omega)$.

If the impulsive source is below the reflector, it will produce an out-going wave $\frac{\rho_1 e^{ik_1|z'-z|}}{2ik_1}$ in the second medium; i.e., the Green's function with homogeneous properties (ρ_1, c_1). After the out-going field is obtained, the reflection in the second medium and the transmission in the first medium can be solved as a classical reflection problem, as is presented in equations (12.5) and (12.8), and the final result is:

$$\frac{1}{\rho_1}G_0^+(z,z',\omega) = \begin{cases} \frac{1-R}{2ik_1}e^{ik_1(z-a)}e^{ik(a-z')} & \texttt{if } (z'<a) \\ \frac{1}{2ik_1}\left(e^{ik_1|z'-z|} - Re^{ik_1(z'+z-2a)}\right) & \texttt{if } (z'>a) \end{cases}, \tag{4.3}$$

where $R = \frac{\rho_1 c_1 - \rho_0 c_0}{\rho_1 c_1 + \rho_0 c_0}$ is the reflection coefficient of a plane wave incident from above. Since $\mathcal{B}$ is the depth of the deeper surface, for our wave-field prediction purpose we have $\mathcal{A} < z < \mathcal{B}$. Consequently, G_0^+ will produce two packets of down-going waves at the deeper surface $\mathcal{B}$: $\frac{\rho_1 e^{ik_1(\mathcal{B}-z)}}{2ik_1}$ (the direct wave or the homogeneous propagation as if the entire space is filled with the second medium) and $-R\frac{\rho_1 e^{ik_1(\mathcal{B}+z-2a)}}{2ik_1}$ (the reflection wave‖).

For $z' > z$, G_0^+ can be expressed as:

$$\frac{e^{ik_1|z'-z|} - Re^{ik_1(z'+z-2a)}}{2ik_1/\rho_1} = \frac{e^{ik_1(z'-z)} - Re^{ik_1(z'+z-2a)}}{2ik_1/\rho_1} = \frac{e^{-ik_1 z} - Re^{ik_1(z-2a)}}{2ik_1/\rho_1}e^{ik_1 z'}.$$

In order to have a Green's function that vanishes at the deeper boundary $z' = \mathcal{B}$, we can introduce a homogeneous solution that cancels with the causal solution. As a result, the desired homogeneous solution, denoted as $\phi(z,z',\omega)$, must be

$$\phi(z,z',\omega) = \frac{Re^{ik_1(z-2a)} - e^{-ik_1 z}}{2ik_1/\rho_1}e^{ik_1 z'} \qquad \texttt{if } (z'>z). \tag{4.4}$$

We denote the amplitude factor of the down-going wave $e^{ik_1 z'}$ as $F_1(z,\omega) = \frac{e^{-ik_1 z} - Re^{ik_1(z-2a)}}{2ik_1/\rho_1}$. Our objective is to produce a homogeneous propagation that will produce $-F_1(z,\omega)e^{ik_1 z'}$ for $z' > z$ that cancels G_0^+ at the deeper boundary $z' = \mathcal{B}$. Since the actual medium has a single invariant velocity c_1 for $z' > a$ and there is no velocity change at the source location, $z' = z$, this implies that it is also the solution for a broader region (i.e., $z' > a$):

$$\phi(z,z',\omega) = \frac{Re^{ik_1(z-2a)} - e^{-ik_1 z}}{2ik_1/\rho_1}e^{ik_1 z'} \qquad \texttt{if } (z'>a). \tag{4.5}$$

With the solution for $z' > a$, the wave propagation for $z' < a$ can be unambiguously solved via boundary conditions detailed in Appendix A. The medium's properties are listed in Table 1, and R is used to denote the reflection coefficient of this model when the incident wave is coming from above:

Depth Range	Velocity	Density
$(-\infty, a)$	c_0	ρ_0
(a, ∞)	c_1	ρ_1

Table 1: The properties of an acoustic medium with a single reflector at depth a.

$R = \frac{\rho_1 c_1 - \rho_0 c_0}{\rho_1 c_1 + \rho_0 c_0}$; other coefficients such as the reflection coefficient from below, and the transmission coefficients, can all be easily expressed as a simple function** of R.

According to the classical reflection problem listed in Appendix A, the incident wave (i.e., for $z' < a$) intended to produce the transmission packet in equation (4.5) for the purpose of canceling the boundary values of G_0^+ at the deeper boundary $z' = \mathcal{B}$ is:

$$\frac{-F_1}{1+R} e^{ik_1 a} e^{ik(z'-a)} = \frac{Re^{ik_1(z-a)} - e^{ik_1(a-z)}}{2ik_1(1+R)/\rho_1} e^{ik(z'-a)}. \tag{4.6}$$

However, the above incident wave will produce a corresponding reflection wave in the upper medium (i.e., $z' < a$) as a byproduct:

$$\frac{-F_1 R}{1+R} e^{ik_1 a} e^{ik(a-z')} = \frac{R^2 e^{ik_1(z-a)} - Re^{ik_1(a-z)}}{2ik_1(1+R)/\rho_1} e^{ik(a-z')}. \tag{4.7}$$

We can summarize the solution below the reflector in equation (4.5) and the solution above the reflector in equations (4.6) and (4.7) to have:

$$\phi(z, z', \omega) = \begin{cases} \frac{Re^{ik_1(z-a)} - e^{ik_1(a-z)}}{2ik_1(1+R)/\rho_1} e^{ik(z'-a)} + \frac{R^2 e^{ik_1(z-a)} - Re^{ik_1(a-z)}}{2ik_1(1+R)/\rho_1} e^{ik(a-z')} & \texttt{if } (z' < a) \\ \frac{Re^{ik_1(z-2a)} - e^{-ik_1 z}}{2ik_1/\rho_1} e^{ik_1 z'} & \texttt{if } (z' > a) \end{cases}. \tag{4.8}$$

Combining equations (4.3) and (4.8), the Green's function that satisfies the Dirichlet and Neumann boundary conditions at the deeper boundary $z' = \mathcal{B}$ is:

$$\frac{1}{\rho_1} G_0^{DN}(z, z', \omega) = \frac{G_0^+(z, z', \omega) + \phi(z, z', \omega)}{\rho_1} = \begin{cases} \frac{1-R}{2ik_1} e^{ik_1(z-a)} e^{ik(a-z')} + \\ \frac{Re^{ik_1(z-a)} - e^{ik_1(a-z)}}{2ik_1(1+R)} e^{ik(z'-a)} + \frac{R^2 e^{ik_1(z-a)} - Re^{ik_1(a-z)}}{2ik_1(1+R)} e^{ik(a-z')} & \texttt{if } (z' < a) \\ \frac{e^{ik_1|z'-z|} - Re^{ik_1(z'+z-2a)}}{2ik_1} + \frac{Re^{ik_1(z-2a)} - e^{-ik_1 z}}{2ik_1} e^{ik_1 z'} & \texttt{if } (z' > a) \end{cases}. \tag{4.9}$$

‖The amplitude factor is $-R$ instead of R since the incident wave comes from the second medium (below) rather than the first medium (above).

**For example, the reflection coefficient from below is $-R$, and the transmission coefficients from above and below are $1 + R$ and $1 - R$, respectively.

The above expression can be simplified as:

$$G_0^{DN}(z,z',\omega) = \begin{cases} \frac{Re^{ik_1(z-a)}-e^{ik_1(a-z)}}{2ik_1(1+R)/\rho_1}e^{ik(z'-a)} + \frac{e^{ik_1(z-a)}-Re^{ik_1(a-z)}}{2ik_1(1+R)/\rho_1}e^{ik(a-z')} & \texttt{if } (z'<a) \\ \frac{e^{ik_1|z'-z|}-e^{ik_1(z'-z)}}{2ik_1/\rho_1} & \texttt{if } (z'>a) \end{cases} . \quad (4.10)$$

The procedure above is shown in Figure 5 in the time domain.

Let us study the vanishing property of G_0^{DN} with the source location z below a reflector. If $z' > z$ (which automatically implies the solution in equation (4.10), since the source is located below the reflector: $z > a$), we have:

$$G_0^{DN}(z,z',\omega) = \frac{e^{ik_1|z'-z|} - e^{ik_1(z'-z)}}{2ik_1/\rho_1} = \frac{e^{ik_1(z'-z)} - e^{ik_1(z'-z)}}{2ik_1/\rho_1} \equiv 0 \quad (4.11)$$

According to equation (4.11), G_0^{DN} for $z > a$ also vanishes in the half-space below the source, which includes $z' = \mathcal{B}$, a behavior demonstrated by G_0^{DN} for $z < a$ as well.

Following the argument for G_0^{DN} for $z < a$, it is obvious that any variations of $c(z')$ below the source location z will not change the value of the Green's function with double vanishing boundary conditions. A very important consequence is that any heterogeneity below the prediction point (i.e., the source depth z) will not have any impact on G_0^{DN} and consequently will not affect the imaging result at z. It is worthwhile to remind the reader that this fact had already been in many publications – for example in "Finite Volume Model for Migration" from Weglein et al. (2011a).

In summary, combining equations (4.1) and (4.10), the frequency domain solution for G_0^{DN} with a single reflector located at depth a is:

$$G_0^{DN}(z,z',\omega) = \begin{cases} \frac{\rho_0}{2ik}\left(e^{ik|z-z'|} - e^{ik(z'-z)}\right) & \texttt{if } (z<a), \\ \frac{\rho_1}{2ik_1}\left(e^{ik_1|z'-z|} - e^{ik_1(z'-z)}\right) & \texttt{if } (a<z' \texttt{ and } a<z), \\ \frac{Re^{ik_1(z-a)}-e^{ik_1(a-z)}}{2ik_1(1+R)/\rho_1}e^{ik(z'-a)} + & \\ \frac{e^{ik_1(z-a)}-Re^{ik_1(a-z)}}{2ik_1(1+R)/\rho_1}e^{ik(a-z')} & \texttt{if } (z'<a \texttt{ and } a<z). \end{cases} \quad (4.12)$$

It can be transformed into the time domain via equation (1.1) to have:

$$
G_0^{DN}(z,z',t) = \begin{cases} \frac{\rho_0 c_0}{2}\left(H\left[t+\frac{z-z'}{c_0}\right] - H\left[t-\frac{|z-z'|}{c_0}\right]\right) & \texttt{if } (z<a), \\ \frac{\rho_1 c_1}{2}\left(H\left[t+\frac{z-z'}{c_1}\right] - H\left[t-\frac{|z-z'|}{c_1}\right]\right) & \texttt{if } (a<z' \texttt{ and } a<z), \\ \frac{\rho_1 c_1}{2(1+R)}\left\{\begin{array}{r} H\left(t+\frac{z'-a}{c_0}+\frac{z-a}{c_1}\right) \\ -H\left(t-\frac{z'-a}{c_0}-\frac{z-a}{c_1}\right) \\ +RH\left(t+\frac{z'-a}{c_0}-\frac{z-a}{c_1}\right) \\ -RH\left(t-\frac{z'-a}{c_0}+\frac{z-a}{c_1}\right) \end{array}\right\} & \texttt{if } (z'<a \texttt{ and } a<z). \end{cases} \tag{4.13}
$$

Another important property of G_0^{DN} for a model with a single reflector is that, from both equations (4.12) and (4.13), G_0^{DN} for $a<z$ and for $a<z'$ is the same even if the single reflector does not exist[††]. Note that in this case the additional heterogeneity (i.e., the single reflector) is outside the interval (z',z), and it is obvious that the geologic complexity beyond the (z',z) zone will not affect the value of G_0^{DN}.

The independence of G_0^{DN} from the heterogeneity outside the interval (z',z) agrees with the WKBJ Green's function. The WKBJ Green's function is derived as an approximate solution for a smoothed medium and is not a function of any heterogeneity outside (z',z).

In the procedure to construct G_0^{DN}, we start from the causal solution in equation (4.3). Here the last term is a reflection resulting from the up-going wave produced by the source. Note that this term is canceled after adding the homogeneous solution ϕ in equation (4.8). Consequently, their sum G_0^{DN} contains no reflection generated from the source.

It is well-known that reflections are omitted in both the WKBJ approximation and in many current seismic imaging procedures that prefer a smooth and reflectionless velocity model. In many current imaging algorithms, the velocity field is smoothed to minimize the reflections caused by the velocity, whereas in the logic for Green's function with double vanishing boundary conditions, the discontinuous model is kept intact. Nevertheless, both approaches yield the same reflectionless conclusion.

The procedure in this section to calculate G_0^{DN} for a simple single-reflector model is already very tedious. The major difficulty is to find a homogeneous solution ϕ that will cancel both the downward reflection originating from the source and the downward propagation of the source below the source location. For more complicated geological models, the procedure will be much more demanding.

Fortunately, a much simpler procedure, easily generalizable to more complicated models, can be derived from the fact that the values of G_0^{DN} are not affected by any heterogeneity outside the interval (z',z).

[††]This solution is the same as in equation (3.1) if (1) c_0 is replaced by c_1, and (2) the trivial density contribution at the source ρ_1 is added. And consequently this solution is equivalent with G_0^{DN} with a homogeneous velocity c_1 and constant density ρ_1 that contains no reflector.

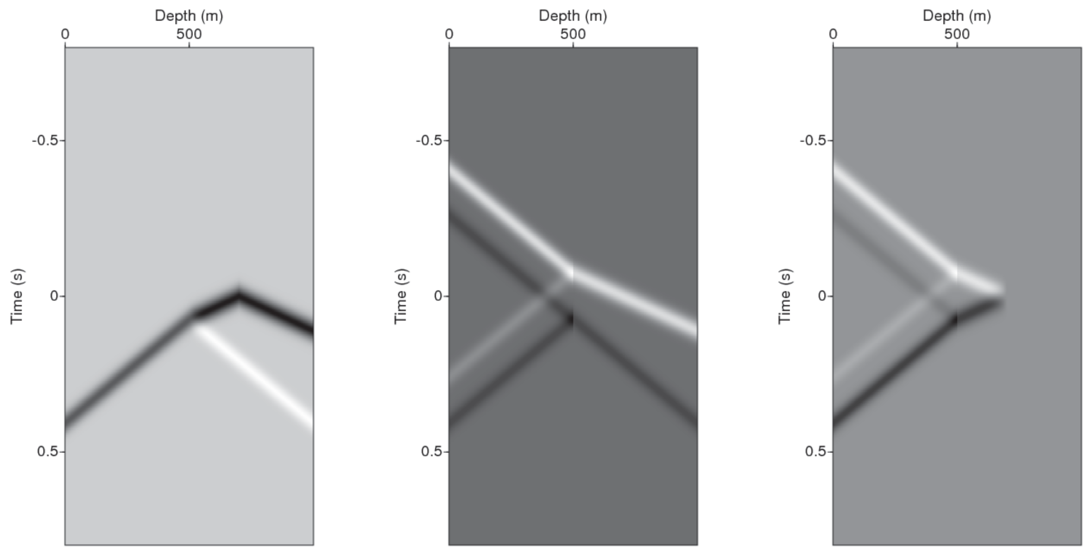

Figure 5: The construction of G_0^{DN} for a medium with one reflector (the velocities above and below the reflector are $1500m/s$ and $2700m/s$, respectively). The source depth is 700m and is below the single reflector at $500m$. The left panel is the causal solution G_0^+, and the middle panel shows the homogeneous solution that cancels with the left panel below the source. The right panel results from summing the two panels on its left and is the desired Green's function with double vanishing boundary conditions.

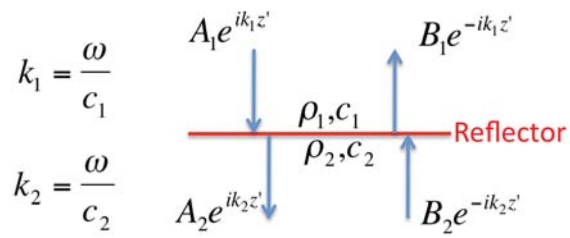

Figure 6: The diagram for upward continuation. A reflector is located at depth a, the medium properties above and below the reflector are (ρ_1, c_1) and (ρ_2, c_2), respectively. In this case we assume that the wave below the reflector $A_2 e^{ik_2 z'} + B_2 e^{-ik_2 z'}$ is known, the objective is to compute the wave above the reflector $A_1 e^{ik_1 z'} + B_1 e^{-ik_1 z'}$.

5 Upward continuation procedure: wave-theory approach

In the process of calculating G_0^{DN} with the source below many reflectors, we start from the wave field of the layer that contains the source. The wave field in this layer can be calculated through equation (4.1), and can be expressed as:

$$A_n e^{ik_n z'} + B_n e^{-ik_n z'},$$

where the source is assumed to be in the $n^{\mathtt{th}}$-layer (with velocity c_n and density ρ_n, respectively), $k_n = \frac{\omega}{c_n}$, $A_n = -\frac{\rho_n}{2ik_n} e^{-iz}$, $B_n = \frac{\rho_n}{2ik_n} e^{iz}$. The objective is to find the wave field at the $(n-1)^{\mathtt{th}}$ layer: $A_{n-1} e^{ik_{n-1} z'} + B_{n-1} e^{-ik_{n-1} z'}$, as shown in Figure 6. The theory is listed below. The continuity of the wave field and its derivatives requires:

$$\begin{aligned} A_1 e^{ik_1 a} + B_1 e^{-ik_1 a} &= A_2 e^{ik_2 a} + B_2 e^{-ik_2 a}, \\ \frac{ik_1}{\rho_1} \left(A_1 e^{ik_1 a} - B_1 e^{-ik_1 a} \right) &= \frac{ik_2}{\rho_2} \left(A_2 e^{ik_2 a} - B_2 e^{-ik_2 a} \right). \end{aligned} \tag{5.1}$$

If we define: $\gamma = \frac{\rho_1 k_2}{\rho_2 k_1} = \frac{\rho_1 c_1}{\rho_2 c_2}$, equation (5.1) can be written in matrix form:

$$\begin{pmatrix} e^{ik_1 a} & -e^{-ik_1 a} \\ e^{ik_1 a} & e^{-ik_1 a} \end{pmatrix} \begin{pmatrix} A_1 \\ B_1 \end{pmatrix} = \begin{pmatrix} \gamma & 0 \\ 0 & 1 \end{pmatrix} \begin{pmatrix} e^{ik_2 a} & -e^{-ik_2 a} \\ e^{ik_2 a} & e^{-ik_2 a} \end{pmatrix} \begin{pmatrix} A_2 \\ B_2 \end{pmatrix}, \tag{5.2}$$

with the solution:

$$\begin{pmatrix} A_1 \\ B_1 \end{pmatrix} = \frac{1}{2}\begin{pmatrix} e^{-ik_1a} & e^{-ik_1a} \\ -e^{ik_1a} & e^{ik_1a} \end{pmatrix}\begin{pmatrix} \gamma & 0 \\ 0 & 1 \end{pmatrix}\begin{pmatrix} e^{ik_2a} & -e^{-ik_2a} \\ e^{ik_2a} & e^{-ik_2a} \end{pmatrix}\begin{pmatrix} A_2 \\ B_2 \end{pmatrix}$$
$$= \frac{1}{2}\begin{pmatrix} \gamma e^{-ik_1a} & e^{-ik_1a} \\ -\gamma e^{ik_1a} & e^{ik_1a} \end{pmatrix}\begin{pmatrix} e^{ik_2a} & -e^{-ik_2a} \\ e^{ik_2a} & e^{-ik_2a} \end{pmatrix}\begin{pmatrix} A_2 \\ B_2 \end{pmatrix} \tag{5.3}$$
$$= \frac{1}{2}\begin{pmatrix} (1+\gamma)e^{i(k_2-k_1)a} & (1-\gamma)e^{-i(k_1+k_2)a} \\ (1-\gamma)e^{i(k_1+k_2)a} & (1+\gamma)e^{i(k_1-k_2)a} \end{pmatrix}\begin{pmatrix} A_2 \\ B_2 \end{pmatrix}.$$

Since $\frac{1+\gamma}{2} = \frac{1}{2} + \frac{\rho_1 c_1}{2\rho_2 c_2} = \frac{\rho_2 c_2 + \rho_1 c_1}{2\rho_2 c_2} = \frac{1}{1+R}$, and $\frac{1-\gamma}{2} = \frac{1}{2} - \frac{\rho_1 c_1}{2\rho_2 c_2} = \frac{\rho_2 c_2 - \rho_1 c_1}{2\rho_2 c_2} = \frac{R}{1+R}$, the above results can be rewritten as:

$$\begin{pmatrix} A_1 \\ B_1 \end{pmatrix} = \frac{1}{1+R}\begin{pmatrix} e^{i(k_2-k_1)a} & Re^{-i(k_1+k_2)a} \\ Re^{i(k_1+k_2)a} & e^{i(k_1-k_2)a} \end{pmatrix}\begin{pmatrix} A_2 \\ B_2 \end{pmatrix}. \tag{5.4}$$

For example, for G_0^{DN} with $z > a$, the wave field immediately below the single reflector is $\frac{\rho_1}{2ik_1}\left(-e^{ik_1(z'-z)} + e^{ik_1(z-z')}\right)$. If it is expressed in the form $A_2 e^{ik_1z'} + B_2 e^{-ik_1z'}$, we have $A_2 = -\frac{\rho_1 e^{-ik_1z}}{2ik_1}$, $B_2 = \frac{\rho_1 e^{ik_1z}}{2ik_1}$ and consequently we have:

$$\begin{pmatrix} A_1 \\ B_1 \end{pmatrix} = \frac{1}{1+R}\begin{pmatrix} e^{i(k_1-k)a} & Re^{-i(k+k_1)a} \\ Re^{i(k+k_1)a} & e^{i(k-k_1)a} \end{pmatrix}\frac{\rho_1}{2ik_1}\begin{pmatrix} -e^{-ik_1z} \\ e^{ik_1z} \end{pmatrix}$$
$$= \frac{\rho_1}{2ik_1}\frac{1}{1+R}\begin{pmatrix} \left\{Re^{ik_1(z-a)} - e^{ik_1(a-z)}\right\}e^{-ika} \\ \left\{e^{ik_1(z-a)} - Re^{ik_1(a-z)}\right\}e^{ika} \end{pmatrix}. \tag{5.5}$$

From equation (5.5), we can easily produce the wave field above the reflector: $A_1 e^{ikz'} + B_1 e^{-ikz'} = \frac{\rho_1}{2ik_1}\frac{\left\{Re^{ik_1(z-a)} - e^{ik_1(a-z)}\right\}e^{ik(z'-a)} + \left\{e^{ik_1(z-a)} - Re^{ik_1(a-z)}\right\}e^{ik(a-z')}}{1+R}$.

Compared with the previous section, the example above is a much simpler derivation of G_0^{DN} with a single reflector above the source.

For example, for G_0^{DN} in a two-reflector model, the wave field immediately below the second reflector is $A_3 e^{ik_2z'} + B_3 e^{-ik_2z'} = \frac{\rho_2}{2ik_2}\left(-e^{ik_2(z'-z)} + e^{ik_2(z-z')}\right)$. It is obvious that in this case $A_3 = -\frac{\rho_2 e^{-ik_2z}}{2ik_2}$, $B_2 = \frac{\rho_2 e^{ik_2z}}{2ik_2}$ and consequently, we have:

$$\begin{pmatrix} A_2 \\ B_2 \end{pmatrix} = \frac{1}{1+R_2} \begin{pmatrix} e^{i(k_2-k_1)a_2} & R_2 e^{-i(k_1+k_2)a_2} \\ R_2 e^{i(k_1+k_2)a_2} & e^{i(k_1-k_2)a_2} \end{pmatrix} \frac{\rho_2}{2ik_2} \begin{pmatrix} -e^{-ik_2 z} \\ e^{ik_2 z} \end{pmatrix}$$
$$= \frac{\rho_2}{2ik_2} \frac{1}{1+R_2} \begin{pmatrix} \left\{R_2 e^{ik_2(z-a_2)} - e^{ik_2(a_2-z)}\right\} e^{-ik_1 a_2} \\ \left\{e^{ik_2(z-a_2)} - R_2 e^{ik_2(a_2-z)}\right\} e^{ik_1 a_2} \end{pmatrix}. \tag{5.6}$$

Renaming $R = R_1$, and $a = a_1$, the combination of equations (5.4) and (5.6) gives:

$$\begin{pmatrix} A_1 \\ B_1 \end{pmatrix} = \frac{1}{1+R_1} \begin{pmatrix} e^{i(k_1-k)a_1} & R_1 e^{-i(k+k_1)a_1} \\ R_1 e^{i(k+k_1)a_1} & e^{i(k-k_1)a_1} \end{pmatrix} \begin{pmatrix} A_2 \\ B_2 \end{pmatrix}$$
$$= \frac{\rho_2/(1+R_2)}{2ik_2(1+R_1)} \begin{pmatrix} e^{i(k_1-k)a_1} & R_1 e^{-i(k+k_1)a_1} \\ R_1 e^{i(k+k_1)a_1} & e^{i(k-k_1)a_1} \end{pmatrix} \begin{pmatrix} \left\{R_2 e^{ik_2(z-a_2)} - e^{ik_2(a_2-z)}\right\} e^{-ik_1 a_2} \\ \left\{e^{ik_2(z-a_2)} - R_2 e^{ik_2(a_2-z)}\right\} e^{ik_1 a_2} \end{pmatrix}$$
$$= \frac{\rho_2}{2ik_2(1+R_1)(1+R_2)} \times$$
$$\begin{pmatrix} \left[e^{ik_1(a_1-a_2)} \left\{R_2 e^{ik_2(z-a_2)} - e^{ik_2(a_2-z)}\right\} + e^{ik_1(a_2-a_1)} \left\{R_1 e^{ik_2(z-a_2)} - R_1 R_2 e^{ik_2(a_2-z)}\right\}\right] e^{-ika_1} \\ \left[e^{ik_1(a_1-a_2)} \left\{R_1 R_2 e^{ik_2(z-a_2)} - R_1 e^{ik_2(a_2-z)}\right\} + e^{ik_1(a_2-a_1)} \left\{e^{ik_2(z-a_2)} - R_2 e^{ik_2(a_2-z)}\right\}\right] e^{ika_1} \end{pmatrix}. \tag{5.7}$$

If we define: $\lambda \equiv e^{ik_2(z-a_2)}$, $\mu \equiv e^{ik(z'-a_1)}$ and $\nu \equiv e^{ik_1(a_2-a_1)}$, the Green's function can be expressed as:

$$\frac{\left[\nu^{-1}(R_2\lambda - \lambda^{-1}) + R_1\nu(\lambda - R_2\lambda^{-1})\right]\mu + \left[R_1\nu^{-1}(R_2\lambda - \lambda^{-1}) + \nu(\lambda - R_2\lambda^{-1})\right]\mu^{-1}}{2ik_2(1+R_1)(1+R_2)/\rho_2} \tag{5.8}$$

6 Upward continuation: finite-difference approach

In order to demonstrate the general philosophy of our method, we study wave propagation in an arbitrary acoustic medium $c(z)$ (with only velocity variation). It can be extended to a medium with density variation as well. First we have the equation for the causal Green's function with source located at depth z_s:

$$\left(\frac{\partial^2}{\partial z^2} - \frac{1}{c^2(z)}\frac{\partial^2}{\partial t^2}\right) G_0^+(z, z_s, t) = \delta(z - z_s)\delta(t). \tag{6.1}$$

We then consider a homogeneous equation (without the source) in the same velocity field $c(z)$:

$$\left(\frac{\partial^2}{\partial z^2} - \frac{1}{c^2(z)}\frac{\partial^2}{\partial t^2}\right)\phi(z,t) = 0. \tag{6.2}$$

Note that for a small positive number ε, and for $z > z_s + \varepsilon$, the source term of equation (6.1) vanishes: $\delta(z - z_s)\delta(t) = 0$. Consequently, equation (6.1) is a homogeneous wave equation for $z > z_s + \varepsilon$, i.e., identical to equation (6.2).

In the aforementioned source-free region, the difference scheme (with second-order accuracy in both space and time) is:

$$\frac{\phi_{m+1,n} + \phi_{m-1,n} - 2\phi_{m,n}}{(\Delta z)^2} - \frac{1}{c^2}\frac{\phi_{m,n+1} + \phi_{m,n-1} - 2\phi_{m,n}}{(\Delta t)^2} = 0, \tag{6.3}$$

where in the subscript, the variable m denotes the index for depth z, and the variable n denotes the index for time t: $\phi_{m,n} = \phi(m\Delta z, n\Delta t)$. If we define $p \stackrel{\Delta}{=} \frac{c\Delta t}{\Delta z}$, we have:

$$\phi_{m,n+1} = (2 - 2p^2)\phi_{m,n} - \phi_{m,n-1} + p^2(\phi_{m+1,n} + \phi_{m-1,n}), \tag{6.4}$$

for forward marching in time, and

$$\phi_{m-1,n} = (2 - 2p^{-2})\phi_{m,n} - \phi_{m+1,n} + p^{-2}(\phi_{m,n+1} + \phi_{m,n-1}), \tag{6.5}$$

for upward marching in depth. Since both difference schemes with second-order accuracy in equations (6.4) and (6.5) are of the same type, according to the analysis in Alford et al. (1974), equation (6.4) is stable for $\frac{c\Delta t}{\Delta z} \leq \sqrt{0.5}$, and equation (6.5) is stable for $\frac{c\Delta t}{\Delta z} \geq \sqrt{2}$.

Since the value of $G_0^{DN}(z, z')$ is completely determined by the medium in the interval (z', z), if the medium between z' and z is homogeneous, we can extend the local homogeneous medium to the entire space and we have a much simpler problem already solved in equation (14) of Weglein et al. (2011b). In equation (6.5), the initial values are listed on the right-hand side of the formula, with depth levels that have indices m and $m + 1$, respectively. The field values for the depth level with index $m - 1$ can be straightforwardly computed by using equation (6.5), and by using the values at depth indices $m - 1$ and m, the field at depth index $m - 2$ can be likewise calculated. That procedure is very similar to the scheme popularly implemented in finite-difference forward-modeling algorithms that march forward in time.

The two levels of initial field values are from equation (14) of Weglein et al. (2011b), which satisfies the double vanishing Green's function at the lower boundary. These initial field values will not be changed by the scheme in equation (6.5); all the complexity to match the boundary conditions at the current level is carried on to the next depth level with index $m - 1$. It guarantees that both Dirichlet and Neumann boundary conditions at $z' = \mathcal{B}$ are satisfied.

Note that in equation (6.5), the velocity field c is a function of depth and can be arbitrary, enabling the flexibility of the scheme for a medium with any spatially varying velocities.

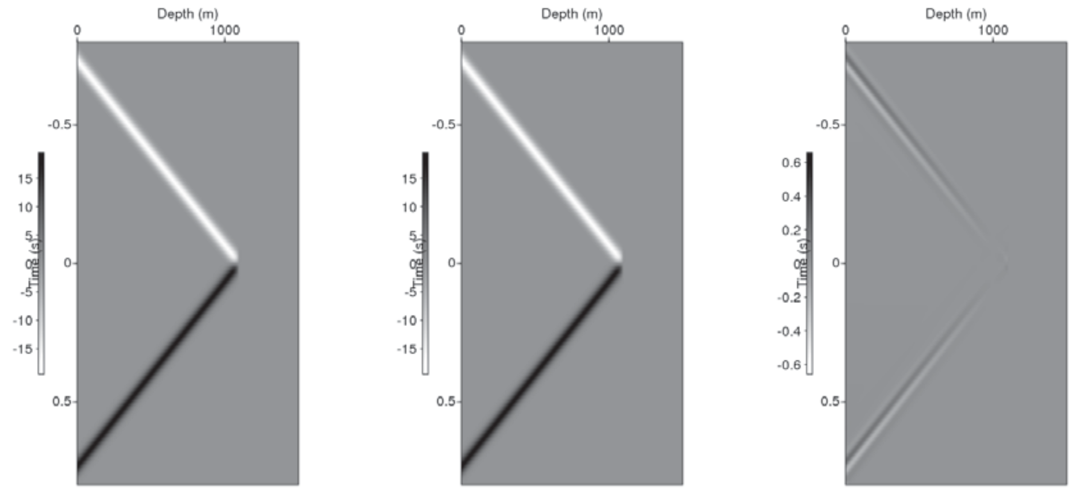

Figure 7: $G_0^{DN}(z = 1100m, z', t)$ for a homogeneous medium with velocity $1500m/s$. The left panel is generated through the finite-difference scheme from equation (6.5). The middle panel is computed from the analytic method and is presented in equation (4.1). The difference between the left and middle panels is shown in the right panel.

7 G_0^{DN} for a model with two reflectors

The G_0^{DN} in this case is for the medium listed in Table 2. The final result is:

$$G_0^{DN}(z,z',\omega) = \begin{cases} \frac{\rho_0}{2ik}\left(e^{ik|z-z'|} - e^{ik(z'-z)}\right) & \texttt{if } (z < a_1) \\ \frac{\rho_1}{2ik_1}\left(e^{ik_1|z'-z|} - e^{ik_1(z'-z)}\right) & \texttt{if } (z' > a_1 \texttt{ and } a_1 < z < a_2) \\ \frac{R_1 e^{ik_1(z-a_1)} - e^{ik_1(a_1-z)}}{2ik_1(1+R_1)/\rho_1} e^{ik_1(z'-a_1)} + & \\ \frac{e^{ik_1(z-a_1)} - R_1 e^{ik_1(a_1-z)}}{2ik_1(1+R_1)/\rho_1} e^{ik_1(a_1-z')} & \texttt{if } (z' < a_1 \texttt{ and } a_1 < z < a_2), \\ \frac{\rho_2}{2ik_2}\left(e^{ik_2|z-z'|} - e^{ik_2(z'-z)}\right) & \texttt{if } (a_2 < z' \texttt{ and } a_2 < z), \\ \frac{R_2 e^{ik_2(z-a_2)} - e^{ik_2(a_2-z)}}{2ik_1(1+R_2)/\rho_2} e^{ik_1(z'-a_2)} + & \\ \frac{e^{ik_2(z-a_2)} - R_2 e^{ik_2(a_2-z)}}{2ik_1(1+R_2)/\rho_2} e^{ik_1(a_2-z')} & \texttt{if } (a_1 < z' < a_2 \texttt{ and } a_2 < z), \\ \frac{\rho_2}{2i(1+R_1)(1+R_2)} \left\{ \begin{array}{r} \nu^{-1}(R_2\lambda - \lambda^{-1})\mu \\ +R_1\nu(\lambda - R_2\lambda^{-1})\mu \\ +R_1\nu^{-1}(R_2\lambda - \lambda^{-1})\mu^{-1} \\ +\nu(\lambda - R_2\lambda^{-1})\mu^{-1} \end{array} \right\} & \texttt{if } (a_2 < z \texttt{ and } z' < a_1). \end{cases} \tag{7.1}$$

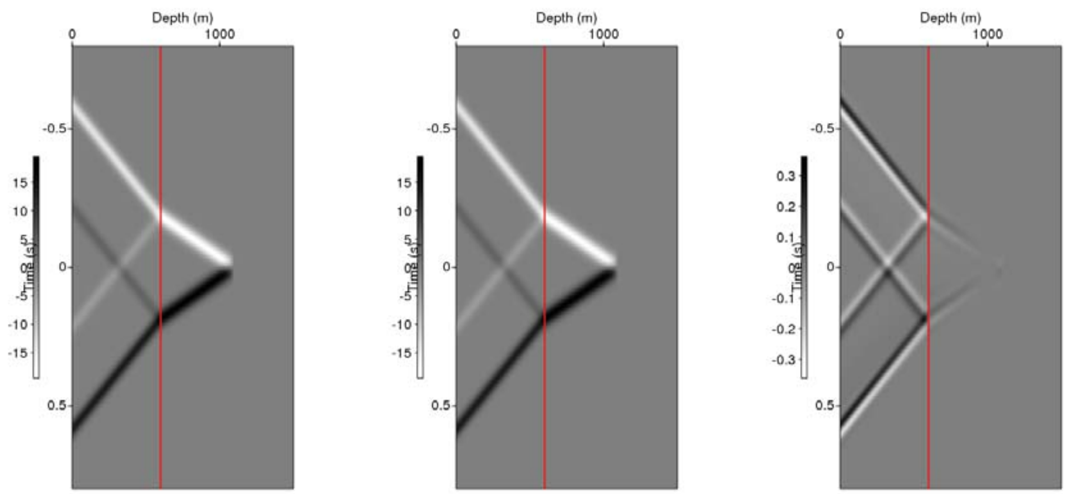

Figure 8: $G_0^{DN}(z = 1100m, z', t)$ for a medium with a reflector at a depth of $600m$. The velocities above and below the reflector are $1500m/s$ and $2700m/s$, respectively. The left panel is generated through the finite-difference scheme from equation (6.5). The middle panel is computed from the analytic method and is presented in equation (4.10). The difference between the left and middle panels is shown in the right panel.

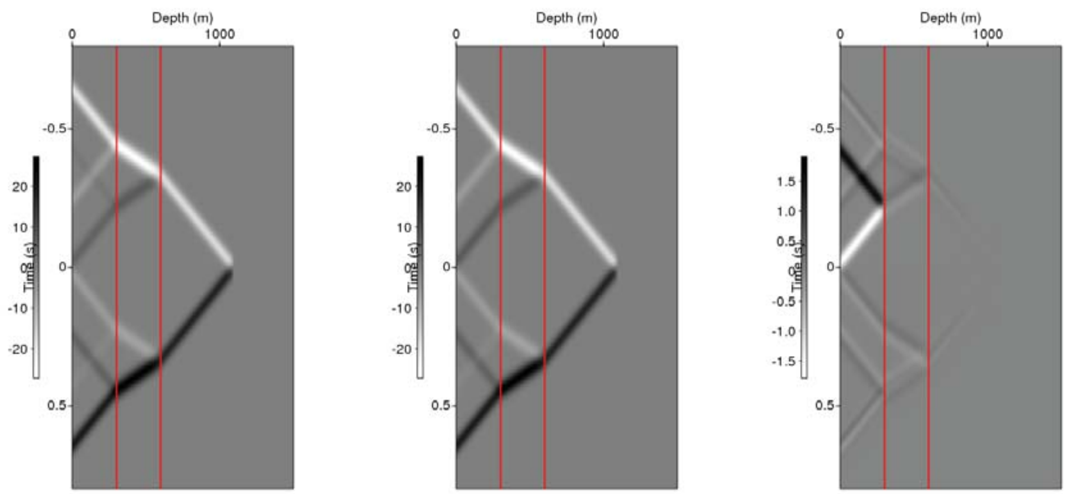

Figure 9: $G_0^{DN}(z = 1100m, z', t)$ for a medium with two reflectors, located at depths of $300m$ and $600m$, respectively. The medium velocities are (from top to bottom) $1500m/s$, $2700m/s$, and $1500m/s$. The left panel is generated through the finite-difference scheme from equation (6.5). The middle panel is computed from the analytic method and is presented in equation (7.1). The difference between the left and middle panels is shown in the right panel.

In the equation above: $\lambda \equiv e^{ik_2(z-a_2)}$, $\mu \equiv e^{ik(z'-a_1)}$, and $\nu \equiv e^{ik_1(a_2-a_1)}$. The details of the above result are listed below:

- Case 1, the source is above the first reflector (i.e., $z < a_1$): the solution in this case is essentially for a whole-space homogeneous medium with velocity c_0 and density ρ_0. The Green's function in this case is the simplest (identical to that for equation (4.1)) and has only two events.
- Case 2, the source is between the first and second reflectors and the receiver is below the first reflector (i.e., $a_1 < z < a_2$ and $a_1 < z'$): the solution in this case is exactly the same as that for a simpler medium that lacks the shallower reflector. It is obtained from equation (4.1), with (c_0, ρ_0) being replaced by (c_1, ρ_1), or the second case of equation (4.10). The G_0^{DN} in this case has two events.
- Case 3, the source is between the first and second reflectors and the receiver is above the first reflector (i.e., $a_1 < z < a_2$ and $z' a_1$. It is the first case of equation (4.10). The G_0^{DN} in this case has four events).
- Case 4, the source and receiver are both below the second reflector (i.e., $a_2 < z$ and $a_2 < z'$): the solution in this case is exactly the same as that for a simpler medium that lacks the shallower reflectors. It is obtained from equation (4.1), with (c_0, ρ_0) being replaced by (c_2, ρ_2).
- Case 5, the source is below the second reflector and the receiver is between the first and second reflectors (i.e., $a_2 < z$ and $a_1 < z' < a_2$). It is obtained from equation (4.10) with (c_1, ρ_1) being replaced by (c_2, ρ_2) and with (c_0, ρ_0) being replaced by (c_1, ρ_1). There are four events in this situation.
- Case 6, the source is below the second reflector and the receiver is above the first reflector (i.e., $a_2 < z$ and $z' < a_1$): this is the most complicated situation and contains eight events. It is calculated by using equation (5.7).

8 Wave-field prediction with the RTM Green's function

In this section, we demonstrate the behavior of the Green's function that satisfies both Dirichlet and Neumann boundary conditions at the deeper boundary. The study consists of three geological models with progressive complexity.

8.1 Example I: homogeneous case

This example had already been documented in Appendix A of Weglein et al. (2011b) for an acoustic medium without density variation; it is given here to make a smooth transition into more complicated examples and to demonstrate the impact of density in the algorithms. With $k = \omega/c_0$, the general solution of a wave propagating in the whole space homogeneous medium with velocity c_0 is:

$$P(z',\omega) = \alpha e^{ikz'} + \beta e^{-ikz'}, \tag{8.1}$$

where α and β can be any value. At the measurement surface $z' = \mathcal{A}$, we will detect the wave field and its partial derivative over z' as follows:

$$\begin{aligned} P(z')\Big|_{z'=\mathcal{A}} &= \alpha e^{ik\mathcal{A}} + \beta e^{-ik\mathcal{A}}, \\ \frac{\partial P(z',\omega)}{\partial z'}\Bigg|_{z'=\mathcal{A}} &= ik\left(\alpha e^{ik\mathcal{A}} - \beta e^{-ik\mathcal{A}}\right). \end{aligned} \tag{8.2}$$

From equation (4.1), the values of the Green's function needed on the boundary $z' = \mathcal{A}$ are:

$$\begin{aligned} G_0^{DN}(z,z',\omega)\Big|_{z'=\mathcal{A}} &= \frac{\rho(z)}{2ik}\left[e^{ik|z-z'|} - e^{ik(z'-z)}\right]_{z'=\mathcal{A}} = \frac{\rho_0}{2ik}\left[e^{ik|z-\mathcal{A}|} - e^{ik(\mathcal{A}-z)}\right], \\ \frac{\partial}{\partial z'}G_0^{DN}(z,z',\omega)\Bigg|_{z'=\mathcal{A}} &= \frac{\rho(z)}{2}\left[\mathtt{sgn}(z'-z)e^{ik|z-z'|} - e^{ik(z'-z)}\right]_{z'=\mathcal{A}} \\ &= \frac{\rho_0}{2}\left[\mathtt{sgn}(\mathcal{A}-z)e^{ik|z-\mathcal{A}|} - e^{ik(\mathcal{A}-z)}\right]. \end{aligned} \tag{8.3}$$

Using the boundary values of the wave field P and Green's operator G_0^{DN} at the boundary $z' = \mathcal{A}$ (in equations (8.2) and (8.3)), we can predict the wave field as follows,

$$\begin{aligned} P(z,\omega) =& \frac{1}{\rho(z')}\left[P(z',\omega)\frac{\partial G_0^{DN}(z,z',\omega)}{\partial z'} - G_0^{DN}(z,z',\omega)\frac{\partial P(z',\omega)}{\partial z'}\right]_{z'=\mathcal{A}}^{z'=\mathcal{B}} \\ =& -\frac{1}{\rho_0}\left[P(z',\omega)\frac{\partial G_0^{DN}(z,z',\omega)}{\partial z'} - G_0^{DN}(z,z',\omega)\frac{\partial P(z',\omega)}{\partial z'}\right]_{z'=\mathcal{A}} \\ =& -\frac{\alpha e^{ik\mathcal{A}} + \beta e^{-ik\mathcal{A}}}{2}\left[\mathtt{sgn}(\mathcal{A}-z)e^{ik|z-\mathcal{A}|} - e^{ik(\mathcal{A}-z)}\right] \\ &+ \frac{\alpha e^{ik\mathcal{A}} - \beta e^{-ik\mathcal{A}}}{2}\left[e^{ik|z-\mathcal{A}|} - e^{ik(\mathcal{A}-z)}\right]. \end{aligned} \tag{8.4}$$

For the purpose of predicting the wave field below the measurement surface $z' = \mathcal{A}$, we obviously have the situation $z > \mathcal{A}$. Consequently, the equation above can be simplified as,

$$\begin{aligned} P(z,\omega) =& \frac{\alpha e^{ik\mathcal{A}} + \beta e^{-ik\mathcal{A}}}{2}\left[e^{ik(z-\mathcal{A})} + e^{ik(\mathcal{A}-z)}\right] + \frac{\alpha e^{ik\mathcal{A}} - \beta e^{-ik\mathcal{A}}}{2}\left[e^{ik(z-\mathcal{A})} - e^{ik(\mathcal{A}-z)}\right] \\ =& \alpha e^{ik\mathcal{A}}e^{ik(z-\mathcal{A})} + \beta e^{-ik\mathcal{A}}e^{ik(\mathcal{A}-z)} \\ =& \alpha e^{ikz} + \beta e^{-ikz}. \end{aligned} \tag{8.5}$$

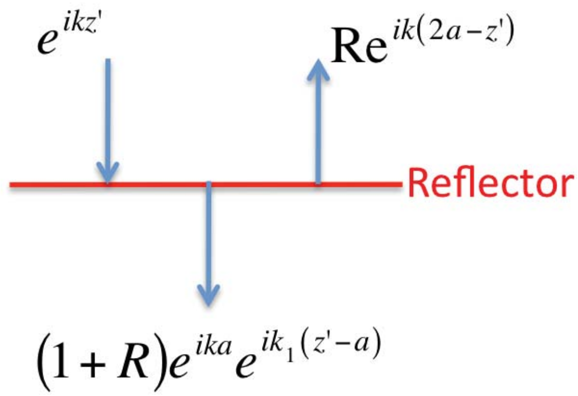

Figure 10: The incident, reflection, and transmission waves in example II. Here $k = \omega/c_0$, $k_1 = \omega/c_1$, and a is the depth of the single reflector. $R = (\rho_1 c_1 - \rho_0 c_0)/(\rho_1 c_1 + \rho_0 c_0)$ is the reflection coefficient for a down-going incident plane wave. $e^{ikz'}$ is the incident wave. $Re^{ik(2a-z')}$ is the reflection data. $(1+R)e^{ika}e^{ik_1(z'-a)}$ is the transmission wave.

The above expression is exactly the actual wave field that we assumed in equation (8.1). In other words, the original wave field, with both up-going and down-going waves, is perfectly reconstructed at an arbitrary depth.

It would sound irrational that we can also perfectly predict the wave field if there are reflectors below z. However, according to d'Alembert's formula for a 1D wave equation for any interval, the introduction of additional reflectors into the homogeneous reference medium below z will not alter the possible type of waves between a and z, which remains homogeneous: $\alpha e^{ikz} + \beta e^{-ikz}$, where α and β are arbitrary numbers. The examples of using this Green's function derived from homogeneous media for nonhomogeneous velocity models can be found in Examples II and III.

8.2 Example II: a single reflector

With the models listed in Table 1, an incident plane wave $e^{ikz'}$ will produce various waves, as shown in Figure 10. Obviously the wave at the measurement surface is:

$$\begin{aligned} P(z' = \mathcal{A}, \omega) &= e^{ik\mathcal{A}} + Re^{ik(2a-\mathcal{A})}, \\ \left.\frac{P(z' = \mathcal{A}, \omega)}{\partial z'}\right|_{z'=\mathcal{A}} &= ik\left(e^{ik\mathcal{A}} - Re^{ik(2a-\mathcal{A})}\right). \end{aligned} \tag{8.6}$$

First let us consider the simpler situation, predicting the wave field above the reflector: $P(z, \omega)$ where $z < a$. The Green's function can be found in equation (4.1). Note that in this case, we use a reflectionless Green's function to downward continue a reflection.

$$
\begin{aligned}
G_0^{DN}(z,z',\omega)\big|_{z'=\mathcal{A}} &= \frac{\rho(z)}{2ik}\left[e^{ik|z-z'|}-e^{ik(z'-z)}\right]_{z'=\mathcal{A}} = \frac{\rho_0}{2ik}\left[e^{ik(z-\mathcal{A})}-e^{ik(\mathcal{A}-z)}\right], \\
\frac{\partial}{\partial z'}G_0^{DN}(z,z',\omega)\bigg|_{z'=\mathcal{A}} &= \frac{\rho_0}{2}\left[-e^{ik(z-\mathcal{A})}-e^{ik(\mathcal{A}-z)}\right].
\end{aligned}
\tag{8.7}
$$

In the equation above, we take advantage of the fact that $\mathtt{sgn}(\mathcal{A}-z)=-1$. With the boundary values from equations (8.6) and (8.7), we can predict the wave field at arbitrary location z using equation (2.5):

$$
\begin{aligned}
P(z,\omega) =& \frac{e^{ik\mathcal{A}}+Re^{ik(2a-\mathcal{A})}}{2}\left[e^{ik(z-\mathcal{A})}+e^{ik(\mathcal{A}-z)}\right]+\frac{e^{ik\mathcal{A}}-Re^{ik(2a-\mathcal{A})}}{2}\left[e^{ik(z-\mathcal{A})}-e^{ik(\mathcal{A}-z)}\right] \\
=& e^{ik\mathcal{A}}e^{ik(z-\mathcal{A})}+Re^{ik(2a-\mathcal{A})}e^{ik(\mathcal{A}-z)} \\
=& e^{ikz}+Re^{ik(2a-z)}.
\end{aligned}
\tag{8.8}
$$

Next let us predict the wave field below the reflector: $P(z,\omega)$, where $z>a$. The value of Green's function at the measurement surface, needed in equation (2.5), can be found in equation (4.10) and is given as:

$$
\begin{aligned}
G_0^{DN}(z,z',\omega)\big|_{z'=\mathcal{A}} &= \frac{\rho_1}{2ik_1}\left\{\frac{R\lambda-\lambda^{-1}}{1+R}\mu+\frac{\lambda-R\lambda^{-1}}{1+R}\mu^{-1}\right\}, \\
\frac{\partial}{\partial z'}G_0^{DN}(z,z',\omega)\bigg|_{z'=\mathcal{A}} &= \frac{\rho_1 k}{2k_1}\left\{\frac{R\lambda-\lambda^{-1}}{1+R}\mu-\frac{\lambda-R\lambda^{-1}}{1+R}\mu^{-1}\right\},
\end{aligned}
\tag{8.9}
$$

where $\lambda \equiv e^{ik_1(z-a)}$ and $\mu \equiv e^{ik(\mathcal{A}-a)}$. With all the terms in equations (8.6) and (8.9), we can predict the wave field below the reflector using equation (2.5):

Depth Range	Velocity	Density
$(-\infty, a_1)$	c_0	ρ_0
(a_1, a_2)	c_1	ρ_1
(a_2, ∞)	c_1	ρ_1

Table 2: The properties of an acoustic medium with two reflectors, at depth a_1 and a_2.

$$\begin{aligned}
P(z,\omega) &= \frac{1}{\rho(z')}\left\{P(z',\omega)\frac{\partial G_0^{DN}(z,z',\omega)}{\partial z'} - G_0^{DN}(z,z',\omega)\frac{\partial P(z',\omega)}{\partial z'}\right\}\Bigg|_{z'=\mathcal{A}}^{z'=\mathcal{B}} \\
&= \frac{1}{\rho(z')}\left[G_0^{DN}(z,z',\omega)\frac{\partial P(z',\omega)}{\partial z'} - P(z',\omega)\frac{\partial G_0^{DN}(z,z',\omega)}{\partial z'}\right]_{z'=\mathcal{A}} \\
&= \frac{\rho_1 k}{\rho_0 k_1}\left\{\frac{\lambda - R\lambda^{-1}}{1+R}\mu^{-1}e^{ik\mathcal{A}} - \frac{R\lambda - \lambda^{-1}}{1+R}\mu R e^{ik(2a-\mathcal{A})}\right\} \\
&= \frac{\rho_1 k}{\rho_0 k_1}e^{ika}\left\{\frac{\lambda - R\lambda^{-1}}{1+R} - \frac{R^2\lambda - R\lambda^{-1}}{1+R}\right\} \\
&= \frac{\rho_1 c_1}{\rho_0 c_0(1+R)}e^{ika}\left\{\left[1-R^2\right]\lambda + \left[R-R\right]\lambda^{-1}\right\} \\
&= \frac{\rho_1 c_1}{\rho_0 c_0}(1-R)\lambda e^{ika} = \frac{\rho_1 c_1}{\rho_0 c_0}\frac{2\rho_0 c_0}{\rho_1 c_1 + \rho_0 c_0}\lambda e^{ika} = \frac{2\rho_1 c_1}{\rho_1 c_1 + \rho_0 c_0}\lambda e^{ika} \\
&= (R+1)\lambda e^{ika} = (1+R)e^{ika}e^{ik_1(z-a)}.
\end{aligned} \tag{8.10}$$

In the derivation above, we take advantage of the fact that $\mu \cdot e^{ik(2a-\mathcal{A})} = \mu^{-1}e^{ik\mathcal{A}} = e^{ika}$. The final result above is exactly the transmission wave in the second medium illustrated in Figure 10. Note that the down-going incident wave and the up-going reflection data act together to produce the down-going transmission data in the second medium, with correct amplitude and phase.

In the G_0^{DN} expression in equation (8.9), the λ terms are for the down-going wave, and the λ^{-1} terms are for the up-going wave. In other words, both down-going and up-going energy is present in the formalism. However, the action of the data cancels the up-going terms (i.e., the terms containing λ^{-1}) in the second medium, as it should.

8.3 Example III: a model with two reflectors: reconstruction of internal multiples in the subsurface

As was chosen in Example II, the incident wave here is $e^{ikz'}$, and the reflection data contain two primaries, corresponding to each reflector, and an infinite number of internal multiples. The measurement at $z' = \mathcal{A}$ is:

$$
\begin{aligned}
P(z'=\mathcal{A},\omega) &= e^{ik\mathcal{A}} + R_1 e^{ik(2a_1-\mathcal{A})} \\
&\quad + \left(1-R_1^2\right) e^{ik(2a_1-\mathcal{A})} \sum_{n=0}^{\infty} (-1)^n R_1^n R_2^{n+1} e^{ik_1(2n+2)[a_2-a_1]}, \\
\frac{1}{ik}\left.\frac{P(z'=\mathcal{A},\omega)}{\partial z'}\right|_{z'=\mathcal{A}} &= e^{ik\mathcal{A}} - R_1 e^{ik(2a_1-\mathcal{A})} \\
&\quad - \left(1-R_1^2\right) e^{ik(2a_1-\mathcal{A})} \sum_{n=0}^{\infty} (-1)^n R_1^n R_2^{n+1} e^{ik_1(2n+2)[a_2-a_1]},
\end{aligned}
\tag{8.11}
$$

where $R_1 = \frac{\rho_1 c_1 - \rho_0 c_0}{\rho_1 c_1 + \rho_0 c_0}$ and $R_2 = \frac{\rho_2 c_2 - \rho_1 c_1}{\rho_2 c_2 + \rho_1 c_1}$ are the reflection coefficients for the first and second reflectors, respectively. Since $1 + R_1$ and $1 - R_1$ are the transmission coefficients for a down-going and an up-going wave through the first reflector, respectively, $1 - R_1^2 = (1 + R_1)(1 - R_1)$ is the total transmission loss for seismic energy passing through the first reflector. To predict the wave field in the second medium (i.e., $a_1 < z' < a_2$), the Green's function can be found in equation (4.12) and is:

$$
\begin{aligned}
\left.G_0^{DN}(z,z',\omega)\right|_{z'=\mathcal{A}} &= \frac{\rho_1}{2ik_1}\left\{\frac{R_1\lambda - \lambda^{-1}}{1+R_1}\mu + \frac{\lambda - R_1\lambda^{-1}}{1+R_1}\mu^{-1}\right\}, \\
\left.\frac{\partial}{\partial z'}G_0^{DN}(z,z',\omega)\right|_{z'=\mathcal{A}} &= \frac{\rho_1 k}{2k_1}\left\{\frac{R_1\lambda - \lambda^{-1}}{1+R_1}\mu - \frac{\lambda - R_1\lambda^{-1}}{1+R_1}\mu^{-1}\right\},
\end{aligned}
\tag{8.12}
$$

where in the equation above $\lambda \equiv e^{ik_1(z-a_1)}$ and $\mu \equiv e^{ik(\mathcal{A}-a_1)}$. With all the terms in equations (8.11) and (9.34), we can predict the wave field below the reflector using equation (2.5):

$$
\begin{aligned}
P(z,\omega) =\ & \frac{1}{\rho(z')}\left\{P(z',\omega)\frac{\partial G_0^{DN}(z,z',\omega)}{\partial z'} - G_0^{DN}(z,z',\omega)\frac{\partial P(z',\omega)}{\partial z'}\right\}\Bigg|_{z'=\mathcal{A}}^{z'=\mathcal{B}} \\
&= \frac{1}{\rho(z')}\left[G_0^{DN}(z,z',\omega)\frac{\partial P(z',\omega)}{\partial z'} - P(z',\omega)\frac{\partial G_0^{DN}(z,z',\omega)}{\partial z'}\right]_{z'=\mathcal{A}} \\
&= \frac{\rho_1 k}{\rho_0 k_1}\left\{\frac{\lambda - R_1\lambda^{-1}}{1+R_1}\mu^{-1}e^{ik\mathcal{A}} - \frac{R_1\lambda-\lambda^{-1}}{1+R_1}\mu R_1 e^{ik(2a_1-\mathcal{A})}\right\} \\
&- \frac{\rho_1 k}{\rho_0 k_1}\left\{\frac{R_1\lambda-\lambda^{-1}}{1+R_1}\mu\left(1-R_1^2\right)e^{ik(2a_1-\mathcal{A})}\sum_{n=0}^{\infty}(-1)^n R_1^n R_2^{n+1} e^{ik_1(2n+2)[a_2-a_1]}\right\} \\
&= \frac{\rho_1 k}{\rho_0 k_1}e^{ika_1}\left\{\frac{\lambda - R_1\lambda^{-1}}{1+R_1} - \frac{R_1^2\lambda - R_1\lambda^{-1}}{1+R_1}\right\} \\
&- e^{ika_1}\frac{\rho_1 k}{\rho_0 k_1}(1-R_1)\left\{R_1\lambda-\lambda^{-1}\right\}\sum_{n=0}^{\infty}(-1)^n R_1^n R_2^{n+1} e^{ik_1(2n+2)[a_2-a_1]} \\
&= \frac{\rho_1 c_1}{\rho_0 c_0(1+R_1)}e^{ika_1}\left\{\left[1-R_1^2\right]\lambda + \left[R_1-R_1\right]\lambda^{-1}\right\} \\
&+ e^{ika_1}\frac{\rho_1 k}{\rho_0 k_1}(1-R_1)\left\{e^{ik_1(a_1-z)} - R_1 e^{ik_1(z-a_1)}\right\}\sum_{n=0}^{\infty}(-1)^n R_1^n R_2^{n+1} e^{ik_1(2n+2)[a_2-a_1]}. \\
&= \frac{\rho_1 c_1}{\rho_0 c_0}(1-R_1)\lambda e^{ika_1} \\
&+ e^{ika_1}\frac{\rho_1 k}{\rho_0 k_1}(1-R_1)\left\{e^{ik_1(a_1-z)} - R_1 e^{ik_1(z-a_1)}\right\}\sum_{n=0}^{\infty}(-1)^n R_1^n R_2^{n+1} e^{ik_1(2n+2)[a_2-a_1]}. \\
&= (1+R_1)e^{ika_1}e^{ik_1(z-a_1)} \\
&+ e^{ika_1}\frac{\rho_1 k}{\rho_0 k_1}(1-R_1)\left\{e^{ik_1(a_1-z)} - R_1 e^{ik_1(z-a_1)}\right\}\sum_{n=0}^{\infty}(-1)^n R_1^n R_2^{n+1} e^{ik_1(2n+2)[a_2-a_1]}.
\end{aligned}
\tag{8.13}
$$

In the derivation above we take advantage of the fact that $\mu e^{ik(2a_1-A)} = e^{ika_1}$. Also, many simplifications are detailed in the process of deriving equation (8.10). Since $\frac{\rho_1 k}{\rho_0 k_1}(1-R_1) = \frac{\rho_1 c_1}{\rho_0 c_0}\frac{2\rho_0 c_0}{\rho_1 c_1+\rho_0 c_0} = \frac{2\rho_1 c_1}{\rho_1 c_1+\rho_0 c_0} = 1+R_1$, the expression above can be simplified as:

$$
\begin{aligned}
P(z,\omega) &= (1+R_1)e^{ika_1}e^{ik_1(z-a_1)} \\
&+ e^{ika_1}(1+R_1)\sum_{n=0}^{\infty}(-1)^n R_1^n R_2^{n+1} e^{ik_1[(2n+2)a_2-(2n+1)a_1-z]} \\
&+ e^{ika_1}(1+R_1)\sum_{n=0}^{\infty}(-1)^{n+1} R_1^{n+1} R_2^{n+1} e^{ik_1[z+(2n+2)a_2-(2n+3)a_1]}.
\end{aligned}
\tag{8.14}
$$

It is very interesting to look each term of the expression above.

- $(1+R_1)e^{ika_1}e^{ik_1(z-a_1)}$ is the down-going wave straight from the source.
- For the simplest case, $n=0$, the results are:

$$e^{ika_1}(1+R_1)R_2e^{ik_1(2a_2-a_1-z)} - e^{ika_1}(1+R_1)R_1R_2e^{ik_1(z+2a_2-3a_1)},$$

  where the first term is the up-going primary reflected from the second reflector, and the second term is the down-going leg of the first-order internal multiple.

- For the case $n=1$, we have:

$$-e^{ika_1}(1+R_1)R_1R_2^2e^{ik_1(4a_2-3a_1-z)} + e^{ika_1}(1+R_1)R_1^2R_2^2e^{ik_1(z+4a_2-5a_1)},$$

  where the first term is the up-going leg of the first-order internal multiple, and the second term is the down-going leg of the second-order internal multiple.

The details to predict the wave field below the second reflector are as follows:

$$\begin{aligned}
G_0^{DN}(z,z',\omega)\big|_{z'=\mathcal{A}} &= \frac{\left[\nu^{-1}(R_2\lambda-\lambda^{-1})+R_1\nu(\lambda-R_2\lambda^{-1})\right]\mu+\left[R_1\nu^{-1}(R_2\lambda-\lambda^{-1})+\nu(\lambda-R_2\lambda^{-1})\right]\mu^{-1}}{2ik_2(1+R_1)(1+R_2)/\rho_2},\\
\frac{\partial}{\partial z'}G_0^{DN}(z,z',\omega)\Big|_{z'=\mathcal{A}} &= \frac{\left[\nu^{-1}(R_2\lambda-\lambda^{-1})+R_1\nu(\lambda-R_2\lambda^{-1})\right]\mu-\left[R_1\nu^{-1}(R_2\lambda-\lambda^{-1})+\nu(\lambda-R_2\lambda^{-1})\right]\mu^{-1}}{2k_2(1+R_1)(1+R_2)/(k\rho_2)},
\end{aligned} \tag{8.15}$$

where $\lambda \equiv e^{ik_2(z-a_2)}$, $\mu \equiv e^{ik(\mathcal{A}-a_1)}$, and $\nu \equiv e^{ik_1(a_2-a_1)}$. The wave field from Example III (i.e., equation (8.11)) can be rewritten as:

$$\begin{aligned}
P(z'=\mathcal{A},\omega) &= e^{ik\mathcal{A}}+R_1e^{ik(2a_1-\mathcal{A})}\\
&\quad+\left(1-R_1^2\right)e^{ik(2a_1-\mathcal{A})}\sum_{n=0}^{\infty}(-1)^nR_1^nR_2^{n+1}\nu^{2n+2},\\
\frac{1}{ik}\left.\frac{P(z'=\mathcal{A},\omega)}{\partial z'}\right|_{z'=\mathcal{A}} &= e^{ik\mathcal{A}}-R_1e^{ik(2a_1-\mathcal{A})}\\
&\quad-\left(1-R_1^2\right)e^{ik(2a_1-\mathcal{A})}\sum_{n=0}^{\infty}(-1)^nR_1^nR_2^{n+1}\nu^{2n+2}.
\end{aligned} \tag{8.16}$$

After obtaining the values of the Green's function and wave field at the shallower boundary, we can use the Green's theorem of equation (2.5), with input from equations (8.15) and (8.16), to predict the wave field below the second reflector:

$$
\begin{aligned}
P(z,\omega) =& \frac{1}{\rho(z')}\left\{P(z',\omega)\frac{\partial G_0^{DN}(z,z',\omega)}{\partial z'} - G_0^{DN}(z,z',\omega)\frac{\partial P(z',\omega)}{\partial z'}\right\}\Bigg|_{z'=\mathcal{A}}^{z'=\mathcal{B}} \\
=& \frac{1}{\rho(z')}\left[G_0^{DN}(z,z',\omega)\frac{\partial P(z',\omega)}{\partial z'} - P(z',\omega)\frac{\partial G_0^{DN}(z,z',\omega)}{\partial z'}\right]_{z'=\mathcal{A}} \\
=& \frac{\rho_2 k}{\rho_0 k_2}e^{ika_1}\frac{R_1\nu^{-1}(R_2\lambda-\lambda^{-1})+\nu(\lambda-R_2\lambda^{-1})}{(1+R_1)(1+R_2)} \\
-& \frac{\rho_2 k}{\rho_0 k_2}e^{ika_1}R_1\frac{\nu^{-1}(R_2\lambda-\lambda^{-1})+R_1\nu(\lambda-R_2\lambda^{-1})}{(1+R_1)(1+R_2)} \\
-& \frac{\rho_2 k}{\rho_0 k_2}e^{ika_1}(1-R_1^2)\sum_{n=0}^{\infty}(-1)^n R_1^n R_2^{n+1}\nu^{2n+2}\frac{\nu^{-1}(R_2\lambda-\lambda^{-1})+R_1\nu(\lambda-R_2\lambda^{-1})}{(1+R_1)(1+R_2)}.
\end{aligned}
\tag{8.17}
$$

Since $\frac{\rho_2 k}{\rho_0 k_2} = \frac{\rho_2 c_2}{\rho_0 c_0} = \frac{\rho_1 c_1}{\rho_0 c_0}\frac{\rho_2 c_2}{\rho_1 c_1} = \frac{1+R_1}{1-R_1}\frac{1+R_2}{1-R_2}$, the equation above can be simplified as:

$$
P(z,\omega) = \frac{e^{ika_1}}{(1-R_1)(1-R_2)}\left(\begin{array}{c}
\left[R_1R_2\nu^{-1}+\nu\right]\lambda \quad - \quad \left[R_1\nu^{-1}+R_2\nu\right]\lambda^{-1} \\
-\left[R_1R_2\nu^{-1}+R_1^2\nu\right]\lambda \quad + \quad \left[R_1\nu^{-1}+R_1^2R_2\nu\right]\lambda^{-1} \\
-(1-R_1^2)\lambda\sum_{n=0}^{\infty}(-1)^n\left[R_1^nR_2^{n+2}\nu^{2n+1}+R_1^{n+1}R_2^{n+1}\nu^{2n+3}\right] \\
+(1-R_1^2)\lambda^{-1}\sum_{n=0}^{\infty}(-1)^n\left[R_1^nR_2^{n+1}\nu^{2n+1}+R_1^{n+1}R_2^{n+2}\nu^{2n+3}\right].
\end{array}\right)
\tag{8.18}
$$

Since

$$
\sum_{n=0}^{\infty}(-1)^n\left[R_1^nR_2^{n+2}\nu^{2n+1}+R_1^{n+1}R_2^{n+1}\nu^{2n+3}\right] = R_2^2\nu + (1-R_2^2)\sum_{n=0}^{\infty}(-1)^nR_1^{n+1}R_2^{n+1}\nu^{2n+3}, \tag{8.19}
$$

and

$$
\sum_{n=0}^{\infty}(-1)^n\left[R_1^nR_2^{n+1}\nu^{2n+1}+R_1^{n+1}R_2^{n+2}\nu^{2n+3}\right] = R_2\nu, \tag{8.20}
$$

equation (9.31) can be simplified as follows:

$$P(z,\omega) = \frac{e^{ika_1}(1-R_1^2)\nu}{(1-R_1)(1-R_2)}\left(\lambda - R_2\lambda^{-1} - R_2^2\lambda + R_2\lambda^{-1} - (1-R_2^2)\lambda\sum_{n=0}^{\infty}(-1)^n R_1^{n+1}R_2^{n+1}\nu^{2n+2}\right)$$
$$= \frac{e^{ika_1}(1-R_1^2)(1-R_2^2)}{(1-R_1)(1-R_2)}\lambda\sum_{n=0}^{\infty}(-1)^n R_1^n R_2^n \nu^{2n+1}$$
$$= (1+R_1)(1+R_2)e^{ika_1}e^{ik_2(z-a_2)}\sum_{n=0}^{\infty}(-1)^n R_1^n R_2^n e^{ik_1(2n+1)(a_2-a_1)}.$$

In the derivation above, we rewrite the trivial quantity 1 as the special case of $(-1)^n R_1^n R_2^n \nu^{2n}$ with $n = 0$. The expression above is exactly the wave field in the deepest layer: only the down-going wave is present with correct amplitude; the up-going waves cancel each other, as actually happened in the subsurface.

9 Downward continuation of both source and receiver

The original Green's theorem in this report is derived to downward continue the wave field (i.e., receivers) to the subsurface over a source-free region. It can also be used to downward continue the sources down to the subsurface by taking advantage of reciprocity: the recording is the same after the source and receiver locations are exchanged.

Assuming we have data on the measurement surface: $D(z_g, z_s)$ (its ω dependency is ignored), we can use $G_0^{DN}(z, z_g)$ to downward continue it from z_g to the target depth z:

$$D(z, z_s) = \frac{1}{\rho(z_g)}\left\{\frac{\partial D(z_g, z_s)}{\partial z_g}G_0^{DN}(z, z_g) - D(z_g, z_s)\frac{\partial G_0^{DN}(z, z_g)}{\partial z_g}\right\}. \tag{9.1}$$

Taking the $\frac{\partial}{\partial z_s}$ operation on equation (9.1), we have a similar procedure to downward continue $\frac{D(z_g,z_s)}{\partial z_s}$ to the subsurface:

$$\frac{\partial D(z, z_s)}{\partial z_s} = \frac{1}{\rho(z_g)}\left\{\frac{\partial^2 D(z_g, z_s)}{\partial z_g \partial z_s}G_0^{DN}(z, z_g) - \frac{\partial D(z_g, z_s)}{\partial z_s}\frac{\partial G_0^{DN}(z, z_g)}{\partial z_g}\right\}. \tag{9.2}$$

With equations (9.1) and (9.2), we downward continue the data D and its partial derivative over z_s to the subsurface location z. According to reciprocity, $D(z, z_s) = E(z_s, z)$, where $E(z_s, z)$ is resulted from exchanging the source and receiver locations in the experiment to generate D at the subsurface. The imaginary data $E(z_s, z)$ can be considered as the recording of receiver at z_s for a source located at z.

For this imaginary experiment, the source is located at depth z, according to the Green's theorem which is derived for a source-free region, we can downward continue the recording at z_s to any depth $Z \leq z$.

In seismic migration, we downward continue $E(z_s, z)$ to the same subsurface depth z with $G_0^{DN}(z, z_s)$ to have an experiment with coincident source and receiver:

$$E(z,z) = \frac{1}{\rho(z_s)}\left\{\frac{\partial E(z_s,z)}{\partial z_s} G_0^{DN}(z,z_s) - E(z_s,z)\frac{\partial G_0^{DN}(z,z_s)}{\partial z_s}\right\}, \\ = \frac{1}{\rho(z_s)}\left\{\frac{\partial D(z,z_s)}{\partial z_s} G_0^{DN}(z,z_s) - D(z,z_s)\frac{\partial G_0^{DN}(z,z_s)}{\partial z_s}\right\}. \tag{9.3}$$

With the value of $D(z, z_s)$ and $\frac{\partial D(z,z_s)}{\partial z_s}$ in equations (9.2) and (9.1), we can simplify equation (9.3) as follows:

$$\rho(z_g)\rho(z_s)E(z,z) = D(z_g,z_s)\frac{\partial G_0^{DN}(z,z_g)}{\partial z_g}\frac{\partial G_0^{DN}(z,z_s)}{\partial z_s} - \frac{\partial D(z_g,z_s)}{\partial z_s}\frac{\partial G_0^{DN}(z,z_g)}{\partial z_g}G_0^{DN}(z,z_s) \\ + \frac{\partial^2 D(z_g,z_s)}{\partial z_g \partial z_s}G_0^{DN}(z,z_g)\,G_0^{DN}(z,z_s) - \frac{\partial D(z_g,z_s)}{\partial z_g}\frac{\partial G_0^{DN}(z,z_s)}{\partial z_s}G_0^{DN}(z,z_g). \tag{9.4}$$

If the $z_s < z_g$ and there is no heterogeneity above z_s, the $\frac{\partial}{\partial z_s}$ operation on $D(z_g, z_s)$ is equivalent to multiplying $-ik$, in this case, equation (9.5) can be simplified further:

$$E(z,z) = -\frac{\frac{\partial G_0^{DN}(z,z_s)}{\partial z_s} + ikG_0^{DN}(z,z_s)}{\rho(z_s)}D(z,z_s).$$

As an example, the data in a 2-reflector model (with an ideal impulsive source located at z_s, the depth of receiver is $z_g > z_s$, the depth of reflector are a_1 and a_2, respectively) can be expressed as:

$$D(z_g,z_s) = \frac{\rho_0}{2ik}\left\{e^{ik(z_g-z_s)} + R_1 e^{ik(2a_1-z_g-z_s)}\right\} \\ + \frac{\rho_0}{2ik}\left\{\left(1-R_1^2\right)e^{ik(2a_1-z_g-z_s)}\sum_{n=0}^{\infty}(-1)^n R_1^n R_2^{n+1} e^{ik_1(2n+2)[a_2-a_1]}\right\}. \tag{9.5}$$

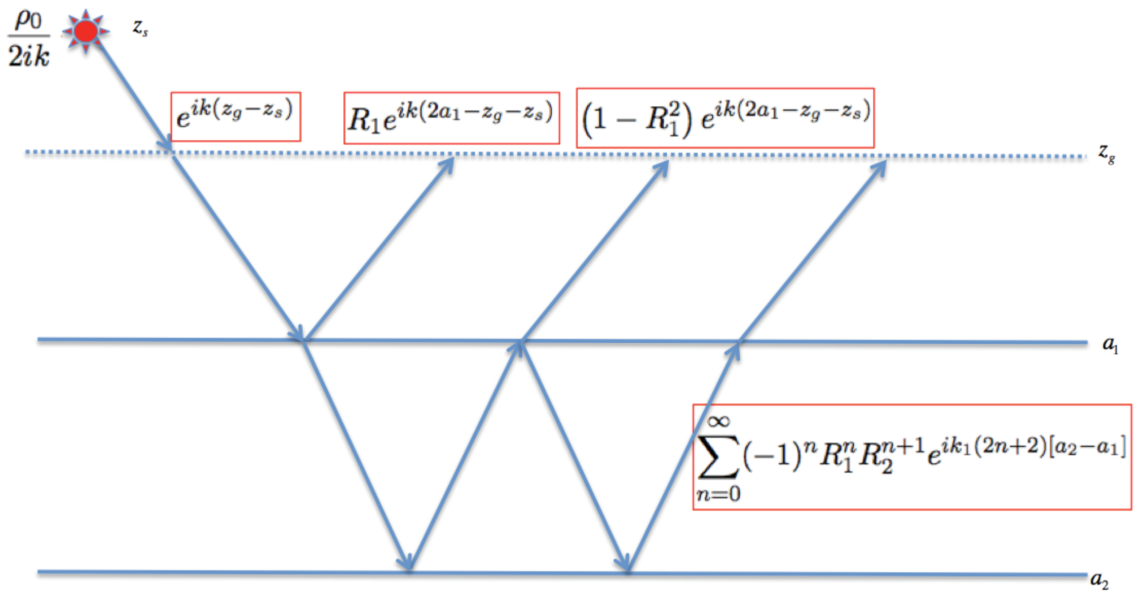

Figure 11: The history of various events in equation (9.5).

If we define $x = e^{ikz_s}$, $y = e^{ikz_g}$, $\sigma = e^{ikz}$, $\beta = \sum_{n=0}^{\infty}(-1)^n R_1^n R_2^{n+1} e^{ik_1(2n+2)[a_2-a_1]}$, and $\alpha = e^{ik(2a_1)}\left(R_1 + (1-R_1^2)\beta\right)$, the data can be expressed as:

$$\begin{aligned}
D(z_g, z_s) &= \frac{\rho_0 x^{-1}}{2ik}\left\{y + \alpha y^{-1}\right\}, \\
\frac{\partial D(z_g, z_s)}{\partial z_g} &= \frac{\rho_0}{2} x^{-1}\left\{y - \alpha y^{-1}\right\}, \\
\frac{\partial D(z_g, z_s)}{\partial z_s} &= -\frac{\rho_0}{2} x^{-1}\left\{y + \alpha y^{-1}\right\}, \\
\frac{\partial^2 D(z_g, z_s)}{\partial z_g \partial z_s} &= \frac{\rho_0 k}{2i} x^{-1}\left\{y - \alpha y^{-1}\right\}.
\end{aligned} \tag{9.6}$$

9.1 Above the first reflector

For $z < a_1$, the boundary values of the Green's function are:

$$\begin{aligned}
G_0^{DN}(z,z_g) &= \rho_0\frac{e^{ik(z-z_g)}-e^{ik(z_g-z)}}{2ik} &&= \rho_0\frac{\sigma y^{-1}-\sigma^{-1}y}{2ik},\\
G_0^{DN}(z,z_s) & &&= \rho_0\frac{\sigma x^{-1}-\sigma^{-1}x}{2ik},\\
\frac{\partial G_0^{DN}(z,z_s)}{\partial z_g} & &&= \rho_0\frac{\sigma y^{-1}+\sigma^{-1}y}{-2},\\
\frac{\partial G_0^{DN}(z,z_s)}{\partial z_s} & &&= \rho_0\frac{\sigma x^{-1}+\sigma^{-1}x}{-2}.
\end{aligned} \tag{9.7}$$

We have:

$$\begin{aligned}
D(z,z_s) &= \frac{G_0^{DN}(z,z_g)\frac{\partial D(z_g,z_s)}{\partial z_g} - \frac{\partial G_0^{DN}(z,z_g)}{\partial z_g}D(z_g,z_s)}{\rho(z_g)}\\
&= \frac{\rho_0 x^{-1}}{4ik}\left(\sigma+\alpha\sigma^{-1}-\sigma^{-1}y^2-\alpha\sigma y^{-2}\right)+\frac{\rho_0 x^{-1}}{4ik}\left(\sigma+\alpha\sigma^{-1}+\sigma^{-1}y^2+\alpha\sigma y^{-2}\right)\\
&= \frac{\rho_0 x^{-1}}{2ik}\left(\sigma+\alpha\sigma^{-1}\right),
\end{aligned} \tag{9.8}$$

and,

$$\frac{-1}{\rho(z_s)}\left(\frac{\partial G_0^{DN}(z,z_s)}{\partial z_s}+ikG_0^{DN}(z,z_s)\right) = \frac{\sigma x^{-1}+\sigma^{-1}x}{2} - \frac{\sigma x^{-1}+\sigma^{-1}x}{2} = \sigma^{-1}x. \tag{9.9}$$

And consequently, we have:

$$\begin{aligned}
E(z,z) &= -\frac{1}{\rho(s)}\left(\frac{\partial G_0^{DN}(z,z_s)}{\partial z_s}+ikG_0^{DN}(z,z_s)\right)D(z,z_s) = \frac{1+\alpha\sigma^{-2}}{2ik/\rho_0}\\
&= \frac{\rho_0}{2ik}\left\{1+e^{ik(2a_1-2z)}\left(R_1+(1-R_1^2)\sum_{n=0}^{\infty}(-1)^n R_1^n R_2^{n+1}e^{ik_1(2n+2)[a_2-a_1]}\right)\right\}.
\end{aligned} \tag{9.10}$$

The result above can be Fourier transformed into the time domain to have:

$$E(z,z,t) = -\frac{\rho_0 c_0}{2}\left\{\begin{array}{l} H(t)+R_1 H\left(t-\frac{2a_1-2z}{c_0}\right)\\ +(1-R_1^2)\sum\limits_{n=0}^{\infty}(-1)^n R_1^n R_2^{n+1} H\left(t-\frac{2a_1-2z}{c_0}-\frac{(2n+2)(a_2-a_1)}{c_1}\right)\end{array}\right\}. \tag{9.11}$$

The terms in the expression above can be interpreted as follows:

- The overall factor $-\frac{\rho_0 c_0}{2}$ is the amplitude of G_0^+ in the first medium.

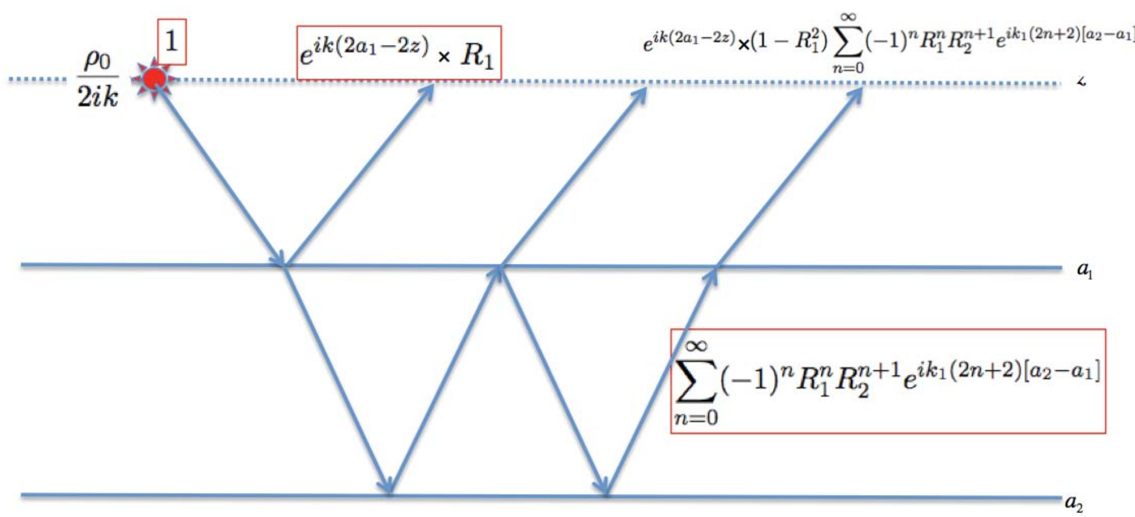

Figure 12: The history of various events in equation (9.10).

- The first term $H(t) = H\left(t - \frac{z-z}{c_0}\right)$ is propagation phase for the direct wave traveling from the source at z to a receiver coincide with the source at z. This term should be removed before applying the imaging condition.
- The second term $R_1 H\left(t - \frac{2a_1-2z}{c_0}\right)$ is the first primary.
- The third term $(1-R_1^2)\sum_{n=0}^{\infty}(-1)^n R_1^n R_2^{n+1} H\left(t - \frac{2a_1-2z}{c_0} - \frac{(2n+2)[a_2-a_1]}{c_1}\right)$ incorporate the second primary and all the internal multiples.

Balancing out the $-\frac{\rho_0 c_0}{2}$ factor, the data after removing the direct wave is denoted as $\mathcal{D}(z,t) \triangleq \frac{-2}{\rho_0 c_0} E(z,z,t) - H(t)$:

$$\mathcal{D}(z,t) = R_1 H\left(t - \frac{2a_1-2z}{c_0}\right) + (1-R_1^2)\sum_{n=0}^{\infty}(-1)^n R_1^n R_2^{n+1} H\left(t - \frac{2a_1-2z}{c_0} - \frac{(2n+2)(a_2-a_1)}{c_1}\right). \tag{9.12}$$

If we use the $t = 0$ imaging condition, we have:

$$\mathcal{D}(z,t) = \begin{cases} 0 & \texttt{if } (z < a_1) \\ R_1 & \texttt{if } (z = a_1) \end{cases} \tag{9.13}$$

In other words, we obtained the image of the first reflector at its actual depth a_1 with its correct reflection coefficient as amplitude.

9.2 Between the first and second reflectors

For $a_1 < z < a_2$, we have:

$$
\begin{aligned}
G_0^{DN}(z, z_g) &= \frac{\rho_1}{2ik_1}\frac{1}{1+R_1}\left((R_1\lambda - \lambda^{-1})\mu + (\lambda - R_1\lambda^{-1})\mu^{-1}\right), \\
\frac{\partial G_0^{DN}(z, z_g)}{\partial z_g} &= \frac{\rho_1 k}{2k_1}\frac{1}{1+R_1}\left((R_1\lambda - \lambda^{-1})\mu - (\lambda - R_1\lambda^{-1})\mu^{-1}\right),
\end{aligned}
\tag{9.14}
$$

where $\lambda = e^{ik_1(z-a_1)}$, $\mu = e^{ik(z_g-a_1)}$. Using equations (9.14) and (9.6), we have:

$$
\begin{aligned}
D(z, z_s) &= \frac{1}{\rho(z_g)}\left(G_0^{DN}(z, z_g)\frac{\partial D(z_g, z_s)}{\partial z_g} - \frac{\partial G_0^{DN}(z, z_g)}{\partial z_g}D(z_g, z_s)\right) \\
&= \frac{\rho_0}{2ik}\frac{\rho_1 k x^{-1}}{\rho_0 k_1(1+R_1)}\left\{(\lambda - R_1\lambda^{-1})\mu^{-1}y - (R_1\lambda - \lambda^{-1})\mu\alpha y^{-1}\right\} \\
&= \frac{\rho_1 x^{-1}}{2ik_1(1+R_1)}\left\{(\lambda - R_1\lambda^{-1})e^{ika_1} - (R_1\lambda - \lambda^{-1})\alpha e^{-ika_1}\right\}
\end{aligned}
\tag{9.15}
$$

If we define: $\beta = \sum_{n=0}^{\infty}(-1)^n R_1^n R_2^{n+1} e^{i(2n+2)[a_2-a_1]}$, we have: $\alpha = e^{2ika_1}\left(R_1 + (1-R_1^2)\beta\right)$, and the equation above can be simplified as:

$$
\begin{aligned}
D(z, z_s) &= \frac{\rho_1 x^{-1}e^{ika_1}}{2ik_1(1+R_1)}\left\{(\lambda - R_1\lambda^{-1}) - (R_1\lambda - \lambda^{-1})\left(R_1 + (1-R_1^2)\beta\right)\right\} \\
&= \frac{\rho_1 x^{-1}e^{ika_1}}{2ik_1}\frac{1-R_1^2}{1+R_1}\left\{\lambda - (R_1\lambda - \lambda^{-1})\beta\right\} \\
&= \frac{\rho_1 x^{-1}e^{ika_1}}{2ik_1}(1-R_1)\left\{\lambda + (\lambda^{-1} - R_1\lambda)\beta\right\} \\
&= \frac{\rho_0}{2ik}x^{-1}e^{ika_1}(1+R_1)\left\{\lambda + (\lambda^{-1} - R_1\lambda)\beta\right\}
\end{aligned}
\tag{9.16}
$$

If we define: $\gamma = 1 - R_1\beta = \sum_{n=0}^{\infty}(-1)^n R_1^n R_2^n e^{ik_1(2n)(a_2-a_1)}$, the expression above can be rewritten as:

$$
D(z, z_s) = \frac{\rho_0}{2ik}(1+R_1)e^{ik(a_1-z)}\left\{\lambda^{-1}\beta + \lambda\gamma\right\}. \tag{9.17}
$$

The expression above can be verified as the following. The overall factor $\frac{\rho_0}{2ik}$ is the amplitude of the G_0^+ at the source. $e^{ik(a_1-z)}$ is the propagation from the source to the first reflector. $1+R_1$ is the transmission coefficient through the first reflector. The first term $\lambda^{-1}\beta$ can be expanded as:

$$\begin{aligned}\lambda^{-1}\beta &= e^{ik_1(a_1-z)}\sum_{n=0}^{\infty}(-1)^n R_1^n R_2^{n+1} e^{ik_1(2n+2)(a_2-a_1)} \\ &= R_2 e^{ik_1(2a_2-a_1-z)} - R_1 R_2^2 e^{ik_1(4a_2-3a_1-z)} + \cdots ,\end{aligned} \tag{9.18}$$

and incorporate all the up-going events. The second term $\lambda\gamma$ can be expanded as:

$$\begin{aligned}\lambda\gamma &= e^{ik_1(z-a_1)}\sum_{n=0}^{\infty}(-1)^n R_1^n R_2^n e^{ik_1(2n)(a_2-a_1)} \\ &= e^{ik_1(z-a_1)} - R_1 R_2 e^{ik_1(z+2a_2-3a_1)} + R_1^2 R_2^2 e^{ik_1(z+4a_2-5a_1)} + \cdots ,\end{aligned} \tag{9.19}$$

and incorporate all the down-going events. And,

$$\begin{aligned}G_0^{DN}(z,z_s) &= \frac{\rho_1}{2ik_1}\frac{1}{1+R_1}\left((R_1\lambda-\lambda^{-1})\xi + (\lambda - R_1\lambda^{-1})\xi^{-1}\right), \\ \frac{\partial G_0^{DN}(z,z_s)}{\partial z_s} &= \frac{\rho_1 k}{2k_1}\frac{1}{1+R_1}\left((R_1\lambda-\lambda^{-1})\xi - (\lambda - R_1\lambda^{-1})\xi^{-1}\right),\end{aligned} \tag{9.20}$$

where $\lambda = e^{ik_1(z-a_1)}$, $\xi = e^{ik(z_s-a_1)}$.

$$\begin{aligned}-\frac{1}{\rho(z_s)}\left(\frac{\partial G_0^{DN}(z,z_s)}{\partial z_s} + ikG_0^{DN}(z,z_s)\right) &= \frac{k\rho_1}{2k_1\rho_0}\frac{(\lambda^{-1}-R_1\lambda)\xi + (R_1\lambda^{-1}-\lambda)\xi^{-1}}{1+R_1} \\ &+ \frac{k\rho_1}{2k_1\rho_0}\frac{(\lambda^{-1}-R_1\lambda)\xi - (R_1\lambda^{-1}-\lambda)\xi^{-1}}{1+R_1} \\ &= \frac{k\rho_1}{k_1\rho_0}\frac{(\lambda^{-1}-R_1\lambda)\xi}{1+R_1}\end{aligned} \tag{9.21}$$

We have:

$$\begin{aligned}&-\frac{1}{\rho(z_s)}\left(\frac{\partial G_0^{DN}(z,z_s)}{\partial z_s} + ikG_0^{DN}(z,z_s)\right)D(z,z_s) = \frac{\rho_1}{2ik_1}\left\{\lambda^{-1}\beta + \lambda\gamma\right\}\left\{\lambda^{-1} - R_1\lambda\right\} \\ &= \frac{\rho_1}{2ik_1}\left\{\beta\lambda^{-2} - R_1\gamma\lambda^2 + \gamma - \beta R_1\right\}\end{aligned} \tag{9.22}$$

Let's check the physical meaning of the terms above. The first term:

$$\begin{aligned}\beta\lambda^{-2} &= \left[\sum_{n=0}^{\infty}(-1)^n R_1^n R_2^{n+1} e^{ik_1(2n+2)(a_2-a1)}\right] e^{ik_1(2a_1-2z)} \\ &= R_2 e^{ik_1(2a_2-2z)} - R_1 R_2^2 e^{ik_1(4a_2-2a_1-2z)} + R_1^2 R_2^3 e^{ik_1(6a_2-4a_1-2z)} + \cdots\end{aligned} \tag{9.23}$$

incorporates the upward reflections (from the second reflector) towards depth z from below (labeled as event 2, 6, 10, $\cdots$ in Figure 13). And the second term :

$$\begin{aligned}-R_1\gamma\lambda^2 &= -R_1\left[\sum_{n=0}^{\infty}(-1)^n R_1^n R_2^n e^{ik_1(2n)(a_2-a_1)}\right] e^{ik_1(2z-2a_1)} \\ &= -R_1 e^{ik_1(2z-2a_1)} + R_1^2 R_2 e^{ik_1(2z+2a_2-4a_1)} - R_1^3 R_2^2 e^{ik_1(2z+4a_2-6z_1)} + \cdots\end{aligned} \tag{9.24}$$

incorporate the downward reflections (from the first reflector) towards depth z from above (labeled as event 1, 5, 9, $\cdots$ in Figure 13). The rest of events can be interpreted as follows:

$$\begin{aligned}\gamma - \beta R_1 = 1 - 2\beta R1 &= 1 - 2R_1 \sum_{n=0}^{\infty}(-1)^n R_1^n R_2^{n+1} e^{ik(2n+2)(a_2-a_1)} \\ &= 1 + 2\left[-R_1 R_2 e^{ik_1(2a_2-2a_1)}\right]^1 + 2\left[-R_1 R_2 e^{ik_1(2a_2-2a_1)}\right]^2 + 2\left[-R_1 R_2 e^{ik_1(2a_2-2a_1)}\right]^3 + \cdots\end{aligned} \tag{9.25}$$

where in the final expression above, the first term 1 is the propagation phase for the direct arrival from the source (this term is a unit since the source and receiver coincide). The second term $2\left[-R_1 R_2 e^{ik(2a_2-2a_1)}\right]^1$ represents two separate propagations labeled as event 3 and 4 in Figure 13, both events with distinct propagation history share the same propagation time. The third term $2\left[-R_1 R_2 e^{ik(2a_2-2a_1)}\right]^2$ represents two separate propagations labeled as event 7 and 8 in Figure 13, and again both events with distinct propagation history share the same propagation time.

The final result can be Fourier transformed into the time domain as:

$$E(z,z,t) = -\frac{\rho_1 c_1}{2}\left\{\begin{array}{l} H(t) + 2\sum\limits_{n=1}^{\infty}(-1)^n R_1^n R_2^n H\left(t - \frac{2n(a_2-a_1)}{c_1}\right) \\ + \sum\limits_{n=0}^{\infty}(-1)^{n+1} R_1^{n+1} R_2^n H\left(t - \frac{2z+2na_2-2(n+1)a_1}{c_1}\right) \\ + \sum\limits_{n=0}^{\infty}(-1)^n R_1^n R_2^{n+1} H\left(t - \frac{2(n+1)a_2-2na_1-2z}{c_1}\right) \end{array}\right\} \tag{9.26}$$

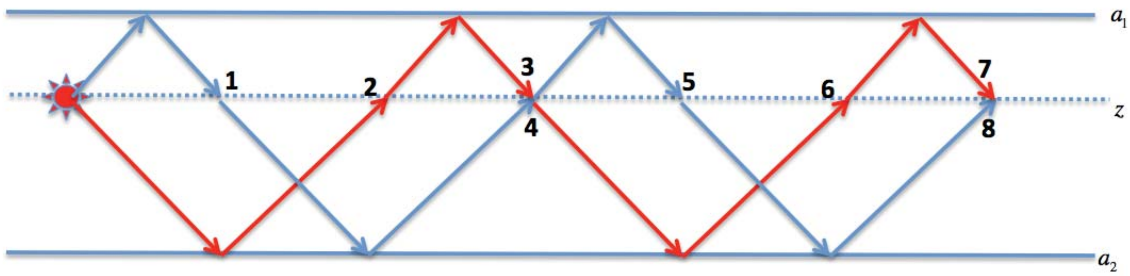

Figure 13: The diagram of events for an experiment with both source and receiver coincide at depth z which located between the first reflector at depth a_1 and the second reflector at depth a_2.

Balancing out the $-\frac{\rho_1 c_1}{2}$ factor, the data after removing the direct wave is denoted as $\mathcal{D}(z,t) \stackrel{\Delta}{=} \frac{-2}{\rho_1 c_1} E(z,z,t) - H(t)$:

$$\mathcal{D}(z,t) = \left\{ \begin{array}{l} 2\sum_{n=1}^{\infty}(-1)^n R_1^n R_2^n H\left(t - \frac{2n(a_2-a_1)}{c_1}\right) \\ + \sum_{n=0}^{\infty}(-1)^{n+1} R_1^{n+1} R_2^n H\left(t - \frac{2z+2na_2-2(n+1)a_1}{c_1}\right) \\ + \sum_{n=0}^{\infty}(-1)^n R_1^n R_2^{n+1} H\left(t - \frac{2(n+1)a_2-2na_1-2z}{c_1}\right) \end{array} \right\} \tag{9.27}$$

and after taking the $t = 0$ imaging condition, we have:

$$\mathcal{D}(z,t) = \begin{cases} -R_1 & \texttt{if } (z = a_1) \\ 0 & \texttt{if } (a_1 < z < a_2) \\ R_2 & \texttt{if } (z = a_2) \end{cases} \tag{9.28}$$

Note that in the previous section, i.e., to image above the first reflector at a_1, we obtain the amplitude R_1 when z approach a_1 from above. In this section we image below the first reflector at a_1, the amplitude of the image is $-R_1$ when z approaches a_1 from below, as it should.

9.3 Below the second reflector

$$\begin{aligned} G_0^{DN}(z,z')\big|_{z'=z_g} &= \frac{\left[\nu^{-1}(R_2\lambda - \lambda^{-1}) + R_1\nu(\lambda - R_2\lambda^{-1})\right]\mu + \left[R_1\nu^{-1}(R_2\lambda - \lambda^{-1}) + \nu(\lambda - R_2\lambda^{-1})\right]\mu^{-1}}{2ik_2(1+R_1)(1+R_2)/\rho_2}, \\ \frac{\partial}{\partial z'} G_0^{DN}(z,z')\Big|_{z'=z_g} &= \frac{\left[\nu^{-1}(R_2\lambda - \lambda^{-1}) + R_1\nu(\lambda - R_2\lambda^{-1})\right]\mu - \left[R_1\nu^{-1}(R_2\lambda - \lambda^{-1}) + \nu(\lambda - R_2\lambda^{-1})\right]\mu^{-1}}{2k_2(1+R_1)(1+R_2)/(k\rho_2)}, \end{aligned} \tag{9.29}$$

where $\lambda \equiv e^{ik_2(z-a_2)}$, $\mu \equiv e^{ik(z_g-a_1)}$, and $\nu \equiv e^{ik_1(a_2-a_1)}$.

$$
\begin{aligned}
D(z,z_s) =& \frac{1}{\rho(z')}\left\{P(z',\omega)\frac{\partial G_0^{DN}(z,z',\omega)}{\partial z'} - G_0^{DN}(z,z',\omega)\frac{\partial P(z',\omega)}{\partial z'}\right\}\Bigg|_{z'=z_g}^{z'=\mathcal{B}} \\
=& \frac{1}{\rho(z')}\left[G_0^{DN}(z,z',\omega)\frac{\partial P(z',\omega)}{\partial z'} - P(z',\omega)\frac{\partial G_0^{DN}(z,z',\omega)}{\partial z'}\right]_{z'=z_g} \\
=& \frac{\rho_2}{2ik_2}e^{ik(a_1-z_s)}\frac{R_1\nu^{-1}(R_2\lambda-\lambda^{-1})+\nu(\lambda-R_2\lambda^{-1})}{(1+R_1)(1+R_2)} \\
&- \frac{\rho_2}{2ik_2}e^{ik(a_1-z_s)}\frac{\nu^{-1}(R_2\lambda-\lambda^{-1})+R_1\nu(\lambda-R_2\lambda^{-1})}{(1+R_1)(1+R_2)}\left\{R_1+(1-R_1^2)\beta\right\}
\end{aligned}
\tag{9.30}
$$

Since $\frac{\rho_2 k}{\rho_0 k_2} = \frac{\rho_2 c_2}{\rho_0 c_0} = \frac{\rho_1 c_1}{\rho_0 c_0}\frac{\rho_2 c_2}{\rho_1 c_1} = \frac{1+R_1}{1-R_1}\frac{1+R_2}{1-R_2}$, the equation above can be simplified as:

$$
D(z,z_s) = \frac{\rho_0 e^{ik(a_1-z_s)}/(2ik)}{(1-R_1)(1-R_2)}
\left(
\begin{array}{c}
\left[R_1R_2\nu^{-1}+\nu\right]\lambda \quad - \quad \left[R_1\nu^{-1}+R_2\nu\right]\lambda^{-1} \\
-\left[R_1R_2\nu^{-1}+R_1^2\nu\right]\lambda \quad + \quad \left[R_1\nu^{-1}+R_1^2R_2\nu\right]\lambda^{-1} \\
-(1-R_1^2)\lambda\sum_{n=0}^{\infty}(-1)^n\left[R_1^nR_2^{n+2}\nu^{2n+1}+R_1^{n+1}R_2^{n+1}\nu^{2n+3}\right] \\
+(1-R_1^2)\lambda^{-1}\sum_{n=0}^{\infty}(-1)^n\left[R_1^nR_2^{n+1}\nu^{2n+1}+R_1^{n+1}R_2^{n+2}\nu^{2n+3}\right].
\end{array}
\right)
\tag{9.31}
$$

Since

$$
\sum_{n=0}^{\infty}(-1)^n\left[R_1^nR_2^{n+2}\nu^{2n+1}+R_1^{n+1}R_2^{n+1}\nu^{2n+3}\right] = R_2^2\nu + (1-R_2^2)\sum_{n=0}^{\infty}(-1)^nR_1^{n+1}R_2^{n+1}\nu^{2n+3}, \tag{9.32}
$$

and

$$
\sum_{n=0}^{\infty}(-1)^n\left[R_1^nR_2^{n+1}\nu^{2n+1}+R_1^{n+1}R_2^{n+2}\nu^{2n+3}\right] = R_2\nu, \tag{9.33}
$$

equation (9.31) can be simplified as follows:

$$
\begin{aligned}
D(z,z_s) &= \frac{\rho_0 e^{ik(a_1-z_s)}(1-R_1^2)\nu}{2ik(1-R_1)(1-R_2)}\left(\lambda - R_2\lambda^{-1} - R_2^2\lambda + R_2\lambda^{-1} - (1-R_2^2)\lambda\sum_{n=0}^{\infty}(-1)^n R_1^{n+1}R_2^{n+1}\nu^{2n+2}\right)\\
&= \frac{\rho_0 e^{ik(a_1-z_s)}(1-R_1^2)(1-R_2^2)}{2ik(1-R_1)(1-R_2)}\lambda\sum_{n=0}^{\infty}(-1)^n R_1^n R_2^n \nu^{2n+1}\\
&= \frac{\rho_0(1+R_1)(1+R_2)}{2ik}e^{ik(a_1-z_s)}e^{ik_2(z-a_2)}\sum_{n=0}^{\infty}(-1)^n R_1^n R_2^n e^{ik_1(2n+1)(a_2-a_1)}.
\end{aligned}
$$

In the derivation above, we rewrite the trivial quantity 1 as the special case of $(-1)^n R_1^n R_2^n \nu^{2n}$ with $n=0$. The expression above is exactly the wave field in the deepest layer: only the down-going wave is present with correct amplitude; the up-going waves cancel with each other as actually happened in the subsurface. And the expression above can be simplified as:

$$
D(z,z_s) = \frac{\rho_0(1+R_1)(1+R_2)}{2ik}e^{ik(a_1-z_s)}e^{ik_1(a_2-a_1)}e^{ik_2(z-a_2)}\gamma
$$

After the downward continuation of the receiver, we can use the Green's theorem to downward continue the source:

$$
\begin{aligned}
G_0^{DN}(z,z')\big|_{z'=z_s} &= \frac{\left[\nu^{-1}(R_2\lambda-\lambda^{-1}) + R_1\nu(\lambda - R_2\lambda^{-1})\right]\xi + \left[R_1\nu^{-1}(R_2\lambda-\lambda^{-1}) + \nu(\lambda - R_2\lambda^{-1})\right]\xi^{-1}}{2ik_2(1+R_1)(1+R_2)/\rho_2},\\
\frac{\partial}{\partial z'}G_0^{DN}(z,z')\bigg|_{z'=z_s} &= \frac{\left[\nu^{-1}(R_2\lambda-\lambda^{-1}) + R_1\nu(\lambda - R_2\lambda^{-1})\right]\xi - \left[R_1\nu^{-1}(R_2\lambda-\lambda^{-1}) + \nu(\lambda - R_2\lambda^{-1})\right]\xi^{-1}}{2k_2(1+R_1)(1+R_2)/(k\rho_2)},
\end{aligned}
\tag{9.34}
$$

where $\lambda \equiv e^{ik_2(z-a_2)}$, $\xi \equiv e^{ik(z_s-a_1)}$, and $\nu \equiv e^{ik_1(a_2-a_1)}$.

$$
-\frac{1}{\rho(z_s)}\left(\frac{\partial G_0^{DN}(z,z_s)}{\partial z_s} + ikG_0^{DN}(z,z_s)\right) = \frac{k\rho_2}{k_2\rho_0}\frac{\nu^{-1}(\lambda^{-1}-R_2\lambda) + R_1\nu(R_2\lambda^{-1}-\lambda)}{(1+R_1)(1+R_2)}\xi,
$$

and

$$
\begin{aligned}
-\frac{1}{\rho(z_s)}\left(\frac{\partial G_0^{DN}(z,z_s)}{\partial z_s} + ikG_0^{DN}(z,z_s)\right)D(z,z_s) = {} & \frac{k\rho_2}{k_2\rho_0}\frac{\nu^{-1}(\lambda^{-1}-R_2\lambda) + R_1\nu(R_2\lambda^{-1}-\lambda)}{(1+R_1)(1+R_2)}e^{ik(z_s-a_1)}\\
& \cdot\frac{\rho_0(1+R_1)(1+R_2)}{2ik}e^{ik(a_1-z_s)}e^{ik_1(a_2-a_1)}e^{ik_2(z-a_2)}\gamma
\end{aligned}
$$

The expression above can be simplified as:

$$
\begin{aligned}
E(z,z) &= \frac{\rho_2}{2ik_2} e^{ik_1(a_2-a_1)} e^{ik_2(z-a_2)} \gamma \left\{ \nu^{-1}(\lambda^{-1} - R_2\lambda) + R_1\nu(R_2\lambda^{-1} - \lambda) \right\} \\
&= \frac{\rho_2}{2ik_2} \nu\lambda\gamma \left\{ \nu^{-1}(\lambda^{-1} - R_2\lambda) + R_1\nu(R_2\lambda^{-1} - \lambda) \right\} \\
&= \frac{\rho_2}{2ik_2} \left\{ 1 - R_2\lambda^2 + R_1R_2\nu^2 - R_1\lambda^2\nu^2 \right\} \gamma \\
&= \frac{\rho_2}{2ik_2} \left\{ 1 + R_1R_2\nu^2 - R_2\lambda^2 - R_1\lambda^2\nu^2 \right\} \gamma
\end{aligned}
$$

Since: $\left(1 + R_1R_2\nu^2\right)\gamma = \left(1 - R_1R_2\nu^2\right) \sum_{n=0}^{\infty} \left[-R_1R_2\nu^2\right]^n = 1$, and:

$$
\begin{aligned}
R_2\lambda^2\gamma &= R_2\lambda^2 \sum_{n=0}^{\infty} (-1)^n R_1^n R_2^n \nu^{2n} = R_2\lambda^2 + R_2\lambda^2 \sum_{n=1}^{\infty} (-1)^n R_1^n R_2^n \nu^{2n} \\
&= R_2\lambda^2 - R_2^2\lambda^2 \sum_{n=1}^{\infty} (-1)^n R_1^n R_2^{n-1} \nu^{2n+2}, \\
R_1\lambda^2\nu^2\gamma &= R_1\lambda^2\nu^2 \sum_{n=0}^{\infty} (-1)^n R_1^n R_2^n \nu^{2n} = \lambda^2 \sum_{n=0}^{\infty} (-1)^n R_1^{n+1} R_2^n \nu^{2n+2}, \\
\left\{ -R_2\lambda^2 - R_1\lambda^2\nu^2 \right\}\gamma &= -R_2\lambda^2 - (1 - R_2^2)\lambda^2 \sum_{n=0}^{\infty} (-1)^n R_1^{n+1} R_2^n \nu^{2n+2}.
\end{aligned}
$$

The final downward continuation result can be expressed as:

$$
\begin{aligned}
E(z,z) &= \frac{\rho_2}{2ik_2} \left\{ 1 - R_2\lambda^2 - (1 - R_2^2)\lambda^2 \sum_{n=0}^{\infty} (-1)^n R_1^{n+1} R_2^n \nu^{2n+2} \right\} \\
&= \frac{\rho_2}{2ik_2} \left\{ 1 - R_2\lambda^2 + (1 - R_2^2)\lambda^2 \sum_{n=0}^{\infty} (-1)^{n+1} R_1^{n+1} R_2^n \nu^{2n+2} \right\} \\
&= \frac{\rho_2}{2ik_2} \left\{ 1 - R_2 e^{ik_2(2z-2a_2)} + (1 - R_2^2) e^{ik_2(2z-2a_2)} \sum_{n=0}^{\infty} (-1)^{n+1} R_1^{n+1} R_2^n e^{ik_1(2n+2)(a_2-a_1)} \right\}.
\end{aligned}
$$

In the results above, $\frac{\rho_2}{2ik_2}$ is the overall amplitude of G_0^+ in the third layer. The first term 1 is the propagation phase of the wave traveling from the source and receiver coincide at depth z. The second term $-R_2 e^{ik_1(2a_2-2a_1)}$ is the reflection from the second reflector at depth a_2 (here it has $-R_2$ as its reflection coefficient since both the source and receiver are located below the reflector).

The third term $(1-R_2^2)e^{ik_1(2a_2-2a_1)}\sum_{n=0}^{\infty}(-1)^{n+1}R_1^{n+1}R_2^n e^{ik_1(2n+2)(a_2-a_1)}$ contains infinite number of internal multiples generated between the first and second reflector.

$$E(z,z,t) = -\frac{\rho_2 c_2}{2}\left\{\begin{array}{l} H(t) - R_2 H\left(t-\frac{2z-2a_2}{c_2}\right) \\ +(1-R_2^2)H\left(t-\frac{2z-2a_2}{c_2}-\frac{(2n+2)(a_2-a_1)}{c_1}\right)\end{array}\right\} \tag{9.35}$$

Balancing out the $-\frac{\rho_2 c_2}{2}$ factor, the data after removing the direct wave is denoted as $\mathcal{D}(z,t) \triangleq \frac{-2}{\rho_2 c_2}E(z,z,t) - H(t)$:

$$\mathcal{D}(z,t) = \left\{\begin{array}{l} -R_2 H\left(t-\frac{2z-2a_2}{c_2}\right) \\ +(1-R_2^2)H\left(t-\frac{2z-2a_2}{c_2}-\frac{(2n+2)(a_2-a_1)}{c_1}\right)\end{array}\right\} \tag{9.36}$$

and after taking the $t=0$ imaging condition, we have:

$$\mathcal{D}(z,t) = \begin{cases} -R_2 & \texttt{if } (z=a_2) \\ 0 & \texttt{if } (a_2<z) \end{cases} \tag{9.37}$$

Note that in the previous section, i.e., to image between the first and second reflectors, we obtain the amplitude R_2 when z approach a_2 from above. In this section we image below the second reflector at a_2, the amplitude of the image is $-R_2$ when z approaches a_2 from below, as it should.

10 Conclusions

A general and efficient procedure to compute the Green's function with vanishing Dirichlet and Neumann boundary conditions has been derived for a 1D medium of arbitrary complexity, and its effectiveness has been demonstrated with numerical examples that accurately predict the up-going and down-going wave field at depth using only the data on the shallower measurement surface. The density contribution to the Green's theorem and Green's function is accurately studied to better understand its role in imaging. In order to generalize the idea in this paper to a multidimensional earth, a finite-difference scheme is derived and validated by comparison with an analytic benchmark.

Several remarkable properties of the Green's function with double vanishing boundary conditions have been identified:

- The vanishing property of G_0^{DN} for $z>a$ unequivocally states that it is not necessary to know the medium's properties below a target to achieve the target's depth image. This conclusion is also stated in the paper "Finite volume model for migration" by Weglein et al. (2011a).

- G_0^{DN} contains no internal multiple and no source-generated reflections; this property agrees perfectly with not only the reflectionless approximation of WKBJ Green's function, but also with the idea of avoiding reflections and multiples in many current seismic imaging procedures.

We also have reported some very early and very positive news on the first wave theory RTM imaging tests, with a discontinuous reference medium and images that have the correct depth and amplitude (that is, producing the reflection coefficient at the correctly located target) with primaries and multiples in the data. That is an implementation of Weglein et al. (2011a;b) with creative implementation and testing and analysis.

11 Acknowledgments

Jim Mayhan and Jinlong Yang provided the proofreading of the manuscript. The authors would like to thank all M-OSRP members and sponsors. This work has been partially funded by NSFCMG award DMS-0327778 and DOE Basic Energy Sciences Award DE-FG02-05ER15697.

12 Appendix A: Classical Reflection Problem

In this appendix we derive and list the solution of the classical acoustic reflection problem. The medium properties are listed in Table 1. We denote $k = \omega/c_0$, $k_1 = \omega/c_1$, and the incident wave is $e^{ikz'}$. We assume the reflection and transmission waves are $Ae^{-ikz'}$ and $Be^{ik_1z'}$, respectively. In order to have a minimal framework for derivation, the philosophy here is to use the simplest possible form for the incident, reflection, and transmission waves. The complexities caused by flexible reflector depth are transferred to the parameters: A and B.

The boundary condition at the boundary $z' = a$ requires that:

$$
\begin{aligned}
e^{ika} + Ae^{-ika} &= Be^{ik_1a}, \\
(ik/\rho_0)e^{ika} + (-ik/\rho_0)Ae^{-ika} &= (ik_1/\rho_1)Be^{ik_1a}.
\end{aligned}
\tag{12.1}
$$

The equations above can be simplified as:

$$
\begin{aligned}
e^{ika} + Ae^{-ika} &= Be^{ik_1a}, \\
e^{ika} - Ae^{-ika} &= \frac{\rho_0 k_1}{\rho_1 k}Be^{ik_1a}.
\end{aligned}
\tag{12.2}
$$

Since $\frac{\rho_0 k_1}{\rho_1 k} = \frac{c_0\rho_0}{c_1\rho_1}$, we have:

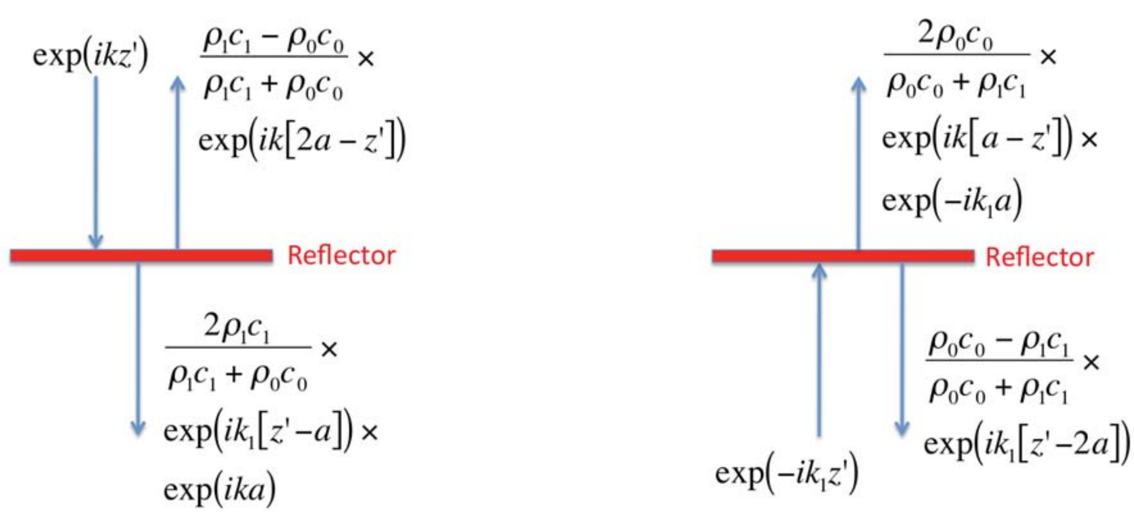

Figure 14: The solution of the two acoustic reflection problems in this appendix. Left: The down-going incident wave from the medium above; right: the up-going incident wave from the medium below.

$$
\begin{aligned}
e^{ika} + Ae^{-ika} &= Be^{ik_1 a}, \\
e^{ika} - Ae^{-ika} &= \frac{\rho_0 c_0}{\rho_1 c_1} Be^{ik_1 a}.
\end{aligned} \tag{12.3}
$$

Solving the above equations, we have:

$$
\begin{aligned}
A &= \frac{c_1\rho_1 - c_0\rho_0}{c_1\rho_1 + c_0\rho_0} e^{ik(2a)} = Re^{ik(2a)}, \\
B &= \frac{2c_1\rho_1}{c_1\rho_1 + c_0\rho_0} e^{i(k-k_1)a} = Te^{i(k-k_1)a}.
\end{aligned} \tag{12.4}
$$

If the incident wave comes from the second medium: $e^{-ik_1 z'}$, similarly we can assume the reflection wave being of the form $Ae^{ik_1 z'}$ and the transmission wave of the form $Be^{-ikz'}$.

$$
\begin{aligned}
e^{-ik_1 a} + Ae^{ik_1 a} &= Be^{-ika}, \\
(-ik_1/\rho_1)e^{-ik_1 a} + (ik_1/\rho_1)Ae^{ik_1 a} &= (-ik/\rho_0)Be^{-ika}.
\end{aligned} \tag{12.5}
$$

After a straightforward simplification we have:

$$
\begin{aligned}
e^{-ik_1a} + Ae^{ik_1a} &= Be^{-ika}, \\
e^{-ik_1a} - Ae^{ik_1a} &= \frac{k\rho_1}{k_1\rho_0}Be^{-ika}.
\end{aligned}
\tag{12.6}
$$

Remove the ω dependency in $\frac{k\rho_1}{k_1\rho_0}$, to have:

$$
\begin{aligned}
e^{-ik_1a} + Ae^{ik_1a} &= Be^{-ika}, \\
e^{-ik_1a} - Ae^{ik_1a} &= \frac{\rho_1 c_1}{\rho_0 c_0}Be^{-ika}.
\end{aligned}
\tag{12.7}
$$

The solution of the above equations is:

$$
\begin{aligned}
A &= \frac{c_0\rho_0 - c_1\rho_1}{c_0\rho_0 + c_1\rho_1}e^{-ik_1(2a)} = Re^{-ik_1(2a)}, \\
B &= \frac{2c_0\rho_0}{c_1\rho_1 + c_0\rho_0}e^{i(k-k_1)a} = Te^{i(k-k_1)a}.
\end{aligned}
\tag{12.8}
$$

13 Appendix B: Confirmation that the Green's function (4.10) is the solution of the wave equation with vanishing Dirichlet and Neumann boundary conditions at the deeper boundary

In this case we have: $\mathcal{A} < a < \mathcal{B}$, and the acoustic wave equation is:

$$
\left\{\rho(z')\frac{\partial}{\partial z'}\left(\frac{\partial}{\rho(z')\partial z'}\right) - \frac{\omega^2}{c^2(z')}\right\} G_0(z, z', \omega) = \delta(z - z'). \tag{13.1}
$$

Here we prove that the boundary conditions at the reflector are satisfied. First is the continuity of pressure. According to equation (4.10), the pressure immediately below the reflector can be obtained by setting z' in the expression for $z' > a$ (i.e., the second case) to a:

$$
G_0(z, a+, \omega) = \rho_1 \frac{e^{ik_1(z-a)} - e^{ik_1(a-z)}}{2ik_1}. \tag{13.2}
$$

while the pressure immediately above the reflector can be obtained by setting z' in the expression for $z' < a$ (i.e., the first case) to a:

$$
G_0(z, a-, \omega) = \frac{\rho_1}{2ik_1}\left\{\frac{Re^{ik_1(z-a)} - e^{ik_1(a-z)}}{1+R} + \frac{e^{ik_1(z-a) - Re^{ik_1(a-z)}}}{1+R}\right\}. \tag{13.3}
$$

We can simplify the expression above as follows:

$$\begin{aligned}
G_0(z, a-, \omega) &= \frac{\rho_1}{2ik_1}\left\{(1-R)e^{ik_1(z-a)} + \frac{-1-R}{1+R}e^{ik_1(a-z)} + \frac{R+R^2}{1+R}e^{ik_1(z-a)}\right\} \\
&= \frac{\rho_1}{2ik_1}\left\{(1-R+R)e^{ik_1(z-a)} - e^{ik_1(a-z)}\right\} \\
&= \frac{\rho_1}{2ik_1}\left\{e^{ik_1(z-a)} - e^{ik_1(a-z)}\right\} \\
&= G_0(z, a+, \omega).
\end{aligned} \tag{13.4}$$

On the other hand, the continuity of $\frac{1}{\rho}\frac{\partial G_0^{DN}}{\partial z'}$ across the boundary can be verified in a similar fashion. The value of $\frac{1}{\rho}\frac{\partial G_0^{DN}}{\partial z'}$ immediately below the reflector is:

$$\frac{1}{\rho_1}\left.\frac{\partial G_0(z, z', \omega)}{\partial z'}\right|_{z'=a+} = \frac{-1}{\rho_1}\left\{e^{ik_1(z-a)} + e^{ik_1(a-z)}\right\}. \tag{13.5}$$

while the value of $\frac{1}{\rho}\frac{\partial G_0^{DN}}{\partial z'}$ immediately above the reflector can be obtained by setting z' in the expression for $z' < a$ (i.e., the first case) to a:

$$\frac{1}{\rho_0}\left.\frac{\partial G_0(z, z', \omega)}{\partial z'}\right|_{z'=a-} = \frac{c_1}{\rho_0 c_0}\left\{\frac{Re^{ik_1(z-a)} - e^{ik_1(a-z)}}{1+R} + \frac{Re^{ik_1(a-z) - e^{ik_1(z-a)}}}{1+R}\right\}. \tag{13.6}$$

We can simplify the expression above as follows:

$$\begin{aligned}
\frac{1}{\rho_0}\left.\frac{\partial G_0(z, z', \omega)}{\partial z'}\right|_{z'=a-} &= \frac{c_1}{\rho_0 c_0}\left\{(R-1)e^{ik_1(z-a)} + \frac{R-R^2}{1+R}e^{ik_1(z-a)} + \frac{R-1}{1+R}e^{ik_1(a-z)}\right\} \\
&= \frac{c_1}{\rho_0 c_0}\left\{\frac{R-1}{R+1}e^{ik_1(z-a)} + \frac{R-1}{R+1}e^{ik_1(a-z)}\right\} \\
&= \frac{c_1}{\rho_0 c_0}\frac{R-1}{R+1}\left\{e^{ik_1(z-a)} + e^{ik_1(a-z)}\right\} \\
&= \frac{-1}{\rho_1}\left\{e^{ik_1(z-a)} + e^{ik_1(a-z)}\right\} \\
&= \frac{1}{\rho_1}\left.\frac{\partial G_0(z, z', \omega)}{\partial z'}\right|_{z'=a+}.
\end{aligned} \tag{13.7}$$

The derivation above takes advantage of the following relations: since $R = \frac{\rho_1 c_1 - \rho_0 c_0}{\rho_1 c_1 + \rho_0 c_0}$, we have:

$$\frac{c_1}{\rho_0 c_0}\frac{R-1}{R+1} = \frac{c_1}{\rho_0 c_0}\frac{\frac{\rho_1 c_1 - \rho_0 c_0}{\rho_1 c_1 + \rho_0 c_0} - 1}{\frac{\rho_1 c_1 - \rho_0 c_0}{\rho_1 c_1 + \rho_0 c_0} + 1} = \frac{c_1}{\rho_0 c_0}\frac{-2\rho_0 c_0}{2\rho_1 c_1} = \frac{-1}{\rho_1}.$$

14 Appendix C: The causal acoustic Green's function used in this report

The analytic solution of the Green's function in equation (2.2) is available if both the velocity $c(z')$ and density $\rho(z')$ fields are constant: i.e., if $c(z') = c_0$ and $\rho(z') = \rho_0$. In this case the term $1/\rho(z') = 1/\rho_0$ becomes a constant and can be moved to the front of the $\partial/\partial z'$ operator, to have:

$$\frac{1}{\rho_0}\left\{\frac{\partial}{\partial z'}\frac{\partial}{\partial z'} + \frac{\omega^2}{c_0^2}\right\} G_0(z, z', \omega) = \delta(z - z').$$

Both terms on the left-hand side of the equation above contain the $\frac{1}{\rho_0}$ factor and the equation can be more succinctly written as:

$$\left\{\frac{\partial}{\partial z'}\frac{\partial}{\partial z'} + \frac{\omega^2}{c_0^2}\right\} G_0(z, z', \omega) = \rho_0 \delta(z - z'). \tag{14.1}$$

Note that the equation above is identical to equation (27) of Weglein et al. (2011a), except for the extra density factor ρ_0 on the right-hand side, and the solution for equation (27) of Weglein et al. (2011a) is $\frac{e^{ik(z-z')}}{2ik}$ where $k = \omega/c_0$; our Green's function in equation (14.1) is:

$$G_0(z, z', \omega) = \frac{\rho_0}{2ik} e^{ik|z-z'|}, \tag{14.2}$$

where again, $k = \omega/c_0$.

References

Alford, R. M., K. R. Kelly, and D. M. Boore. "Accuracy of finite-difference modeling of the acoustic wave equation." Geophysics 39 (1974): 834–842.

Baysal, Edip, Dan D. Kosloff, and John W. C. Sherwood. "Reverse time migration." Geophysics 48 (1983): 1514–1524.

Clayton, R. W. and R. H. Stolt. "A Born-WKBJ inversion method for acoustic reflection data." Geophysics 46 (1981): 1559–1567.

Fletcher, R., P. Fowler, P. Kitchenside, and U. Albertin. "Suppressing unwanted internal reflections in prestack reverse-time migration." Geophysics 71 (2006): E79–E82.

Liu, F., G. Zhang, S. A. Morton, and J. P. Leveille. "An optimized wave equation for seismic modeling and reverse time migration." Geophysics 74 (2009): WCA153–WCA158.

Luo, Yi and Gerard T. Schuster. "Bottom-up target-oriented reverse-time datuming." CPS/SEG Geophysics Conference and Exhibition (2004): F55.

Vigh, Denes, E. William Starr, and Jerry Kapoor. "The role of reverse time migration in complex imaging." CSEG RECORDER (June 2009): 20–24.

Weglein, A. B., R. H. Stolt, and J. D. Mayhan. "Reverse-time migration and Green's theorem: Part I — The evolution of concepts, and setting the stage for the new RTM method." Journal of Seismic Exploration 20 (February 2011): 73–90.

Weglein, A. B., R. H. Stolt, and J. D. Mayhan. "Reverse time migration and Green's theorem: Part II — A new and consistent theory that progresses and corrects current RTM concepts and methods." Journal of Seismic Exploration 20 (May 2011): 135–159.

Whitmore, D. N. "Iterative depth imaging by back time propagation." 53^{rd} Annual International Meeting, SEG, Expanded Abstracts. . Society of Exploration Geophysicists, 1983. 382–385.